



HAL
open science

Evaluation of local friction and pore-water pressure evolution along instrumented probes in saturated clay for large numbers of cycles

Rawaz Dlawar Muhammed, Jean Canou, Jean-Claude Dupla, Alain Tabbagh

► **To cite this version:**

Rawaz Dlawar Muhammed, Jean Canou, Jean-Claude Dupla, Alain Tabbagh. Evaluation of local friction and pore-water pressure evolution along instrumented probes in saturated clay for large numbers of cycles. *Geotechnical and Geological Engineering*, 2019, 56 (12), 10.1139/cgj-2017-0408 . hal-03833022

HAL Id: hal-03833022

<https://hal.science/hal-03833022>

Submitted on 28 Oct 2022

HAL is a multi-disciplinary open access archive for the deposit and dissemination of scientific research documents, whether they are published or not. The documents may come from teaching and research institutions in France or abroad, or from public or private research centers.

L'archive ouverte pluridisciplinaire **HAL**, est destinée au dépôt et à la diffusion de documents scientifiques de niveau recherche, publiés ou non, émanant des établissements d'enseignement et de recherche français ou étrangers, des laboratoires publics ou privés.

Acta Geotechnica

Evolution of cyclic local friction along clay-pile interface for very large numbers of cycles: parametric study --Manuscript Draft--

Manuscript Number:	AGEO-D-19-00017
Full Title:	Evolution of cyclic local friction along clay-pile interface for very large numbers of cycles: parametric study
Article Type:	Original Research Paper
Keywords:	Pile behavior, local shaft friction, amplitude of cyclic loading, frequency, confining effective stress, saturated clay, physical modelling, instrumented pile-probe
Corresponding Author:	Rawaz Dlawar Muhammed, Ph.D Ecole des Ponts ParisTech Champs-sur-Marne, FRANCE
Corresponding Author Secondary Information:	
Corresponding Author's Institution:	Ecole des Ponts ParisTech
Corresponding Author's Secondary Institution:	
First Author:	Rawaz Dlawar Muhammed, Ph.D
First Author Secondary Information:	
Order of Authors:	Rawaz Dlawar Muhammed, Ph.D Jean Canou Jean-Claude Dupla Alain Tabbagh
Order of Authors Secondary Information:	
Funding Information:	
Abstract:	<p>In this paper, an experimental study is presented investigating the influence of cyclic displacement amplitude and effective consolidation stress on the evolution of mobilized local shaft friction along piles submitted to large number of cycles (up to 10^5 cycles). Two-way cyclic displacement-controlled tests were performed on an instrumented pile-probe installed and loaded in a calibration chamber. Tests were performed on reconstituted specimens of saturated clay to examine the shaft friction evolution in the soil-pile interface during cyclic loading. Displacement-controlled static tests were also performed before and after the cyclic loading in order to quantify the influence of cyclic parameters on post-cyclic static response. It was found that the amplitude of cyclic displacement and the initial state of stress have an influence on the evolution of local friction during cyclic loading. The degradation rate of local friction increased for larger cyclic displacement amplitudes whereas with increasing the effective consolidation stress, the degradation rate decreased. The application of displacement- controlled cycles resulted in a modification in the behavior of the interface. A significant peak of static friction followed by strain softening was observed during post cyclic static tests, which was not the case for pre-cyclic static tests. The peak value of friction obtained upon post-cyclic static loadings found to be more important for higher values of applied displacement amplitude during cyclic loading. Finally, a brief synthesis of the results is presented.</p>

[Click here to view linked References](#)

Evolution of cyclic local friction along clay-pile interface for very large numbers of cycles: parametric study

Rawaz Dlawar Muhammed^{1,2}, Jean Canou¹, Jean-Claude Dupla¹, Alain Tabbagh²

¹ *Ecole des Ponts ParisTech, Navier laboratory, France*

² *Pierre and Marie Curie University, France*

Corresponding Author:

Rawaz Dlawar Muhammed

Ecole des Ponts – ParisTech, Navier laboratory

6 – 8 avenue Blaise Pascal, Cité Descartes, Champs-sur-Marne,

77455 Marne-La-Vallée, France

Phone : +33 1 64 15 35 46

Email: rawaz-dlawar.muhammed@enpc.fr

ABSTRACT:

In this paper, an experimental study is presented investigating the influence of cyclic displacement amplitude and effective consolidation stress on the evolution of mobilized local shaft friction along piles submitted to large number of cycles (up to 10^5 cycles). Two-way cyclic displacement-controlled tests were performed on an instrumented pile-probe installed and loaded in a calibration chamber. Tests were performed on reconstituted specimens of saturated clay to examine the shaft friction evolution in the soil-pile interface during cyclic loading. Displacement-controlled static tests were also performed before and after the cyclic loading in order to quantify the influence of cyclic parameters on post-cyclic static response. It was found that the amplitude of cyclic displacement and the initial state of stress have an influence on the evolution of local friction during cyclic loading. The degradation rate of local friction increased for larger cyclic displacement amplitudes whereas with increasing the effective consolidation stress, the degradation rate decreased. The application of displacement- controlled cycles resulted in a modification in the behavior of the interface. A significant peak of static friction followed by strain softening was observed during post cyclic static tests, which was not the case for pre-cyclic static tests. The peak value of friction obtained upon post-cyclic static loadings found to be more important for higher values of applied displacement amplitude during cyclic loading. Finally, a brief synthesis of the results is presented.

KEY WORDS:

Pile behavior, local shaft friction, amplitude of cyclic loading, frequency, confining effective stress, saturated clay, physical modelling, instrumented pile-probe

1 – INTRODUCTION

1
2
3 During their lifetime, pile foundations are often subjected, in addition to permanent static loads,
4 to variable transient loadings, which will sometimes modify their bearing capacity. These
5 complex loadings, often identified under the generic term of “cyclic loadings”, can be
6 characterized by various parameters like the amplitude of the cycles, their frequency, regularity,
7 number of cycles, length of the sequences, etc. Understanding the behavior of piles submitted
8 to such cyclic loadings constitutes an important aspect to be taken into account in the design of
9 pile foundations. Over the past few decades, this subject has attracted considerable scientific
10 interest and numerous research work has been published focusing on pile behavior under cyclic
11 loading (Chan and Hanna [3], Lee and Poulos [9], Al-Douri and Poulos [1], Chin and Poulos
12 [4], Le Kouby et al. [8], Lehane and White [11], Tsuha et al. [23], Poulos [19], Matlock et al.
13 [12], Goulois et al. [6] or Procter and Khaffaf [21]).

14
15
16
17
18 In most laboratory studies based on the use of physical modelling approach of pile-soil interface
19 behavior, the authors usually applied displacement-controlled cyclic loading on their pile,
20 which seems to be the appropriate way to study the evolution of local interface soil-pile friction
21 (ex. Matlock et al. [12], Poulos [20], Procter and Khaffaf [21], Bekki *et al.* [2], Muhammed
22 *et al.* [15]).

23
24
25 Reported studies in the literature showed that the mechanical behavior of the soil–pile interface
26 depends on various parameters like soil, interface and loading parameters. Poulos [19]
27 conducted a number of small-scale laboratory tests on a model pile section (20 mm in diameter)
28 in reconstituted saturated clay specimens (152 mm in diameter), up to maximum number of
29 1000 cycles. According to this author, no degradation of skin friction occurs unless the half-
30 amplitude of the cyclic displacement exceeds about 0.2% of the diameter. Above this value,
31 increasing cyclic displacement amplitude leads to degradation and loss of skin friction. The
32 amplitude of cyclic displacement required to initiate degradation may vary considerably from
33 one test to another. Poulos [20] and Lee and Poulos [10] indicated that the critical amplitude of
34 cyclic displacement, at which cyclic degradation is initiated, is related to the displacement
35 required for full friction mobilization in a static load test.

36
37
38
39
40 All laboratory test results published to date regarding the evolution of local soil-pile interface
41 friction upon cyclic loadings for clays only address small to medium numbers of cycles, less
42 than 10^4 cycles. To the authors’ knowledge, there are no published data showing the influence
43 of cyclic parameters on the evolution of saturated clay-pile local friction for large numbers of
44 cycles. However, in several cases, the foundation of structures can be exposed to cycles of
45 loadings that can exceed 10^4 cycles (ex. offshore wind pile foundation). Investigating the
46 evolution of local pile friction upon large number of cycles is therefore an important issue for
47 better understanding the behavior of piles.

48
49
50
51
52 Within this context, this paper presents the results of an experimental study aimed at better
53 understanding the frictional behavior of a clay-pile interface under large number of cycles. The
54 approach used is of the physical modelling type, using an instrumented prototype probe tested
55 in a calibration chamber and loaded under various types of monotonic and cyclic loadings.

56
57
58
59
60 Based on the results obtained, the influence of cyclic displacement amplitude as well as initial
61 effective consolidation stress of the specimen, on the evolution of mobilized local shaft friction
62 along the probe is investigated for large numbers of cycles (up to 10^5 cycles). Subsequently, the

1 effects of the cyclic sequences on the post-cyclic static response of the pile are presented and
2 discussed.
3
4
5

6 **2 – TESTING SETUP, EXPERIMENTAL PROTOCOLS AND SOIL USED**

7

8
9 The tests presented in this paper have been performed in the calibration chamber available in
10 the geotechnical team of Navier laboratory at Ecole des Ponts ParisTech. The clay specimen is
11 first reconstituted in a large size consolidometer and then transferred onto the calibration
12 chamber for final consolidation. The corresponding detailed experimental protocols used for
13 specimen preparation, application of stresses in the calibration chamber and for carrying out
14 the loading tests with the pile-probe have been fully described by Muhammed [14],
15 Muhammed *et al.* [15] and Muhammed *et al.* [16], who also report on the design of the
16 instrumented pile-probe and the consolidometer. Therefore, a brief description only of the
17 experimental setup and testing protocol is given in the following.
18
19
20
21

22 **2.1 - The calibration chamber testing setup**

23

24
25 A 3D drawing of the calibration chamber test set-up is shown in Fig. 1. The chamber can hold
26 soil specimens 700 mm high and 524 mm in diameter. Independent vertical and horizontal
27 stresses may be applied to the specimens. This allows to apply isotropic or anisotropic initial
28 states of stress or K_0 conditions to the specimens, thus simulating the state of stress applied to
29 a soil element at a given depth. The loading frame of the chamber is equipped with a long stroke
30 classical 100 kN hydraulic jack, used for probe installation at constant displacement rate, and
31 with a servohydraulic 100 kN actuator for carrying out precise displacement-controlled or
32 force-controlled monotonic and cyclic loadings.
33
34
35
36
37

38 **2.2 - Large size consolidometer for reconstituting specimens of saturated fine-grained** 39 **soils**

40

41
42 The consolidometer setup allows to reconstitute, starting from a slurry, saturated clay specimens
43 524 mm in diameter and 600 to 800 mm high under K_0 conditions (no lateral deformation is
44 allowed during the consolidation process). The reservoir of the consolidometer is composed of
45 two Plexiglas adjustable rigid halves equipped with top and bottom draining plates. A loading
46 frame equipped with a double-action hydraulic jack, powered by a hydro-pneumatic pump,
47 allows the application, during the consolidation process, of constant force increments on the
48 top plate of the specimen. Fig. 2 shows a 3D drawing of the consolidometer set-up.
49
50
51
52

53 **2.3 - The instrumented pile-probe**

54

55
56 The prototype probe used allows to make direct and independent measurements of tip resistance
57 and local shaft friction representative of values occurring along a pile shaft. The probe has a
58 cross section of 10 cm² (diameter of 36 mm), similar to standard penetrometers. The conical tip
59
60
61
62

1 of the probe is equipped with a 20 kN precision force transducer and the sleeve, 11 cm long
2 (sleeve surface of 124.4 cm²), is equipped with a ±5 kN force transducer. The bottom part of
3 the probe, including the friction sleeve, is threaded horizontally in order to provide a perfectly
4 rough interface surface state with respect to friction mobilization. The average roughness of the
5 rough part is $R_a = 0.4 \mu\text{m} \pm 0.25$. Fig. 3 shows a simplified cross section of the probe, together
6 with different views.
7

10 2.4 - Experimental procedure

13 *Specimen reconstitution*

15 The specimen preparation comprises two main steps: (1) the specimen is first pre-consolidated
16 in the consolidometer, starting from a clay slurry, to a predefined value of vertical stress, under
17 K_0 conditions; (2) the pre-consolidated specimen is then transferred and positioned on the
18 bottom piston of the calibration chamber and consolidated to the final consolidation stress. The
19 initial water content of the clay slurry has been fixed to about 1.7 times its liquid limit
20 (Muhammed *et al.* [15]). The consolidation of the specimen in the consolidometer is achieved
21 by progressively increasing the vertical load by increments (5, 15, 45, 125, 250, ...kPa) up to
22 the maximum preselected value of the vertical load.
23

24 Once the consolidation process has been completed, the pre-consolidated specimen is
25 transported and carefully adjusted on the bottom piston of the calibration chamber. The
26 consolidation reservoir is taken out and a rubber membrane is adjusted around the clay
27 specimen. The circular confinement wall is then adjusted around the specimen. The final state
28 of consolidation stress can then be slowly applied to the specimen, by increasing independently
29 the vertical pressure within the piston chamber and the lateral confinement pressure. This allows
30 to follow an anisotropic consolidation stress path as the state of stress initially applied in the
31 consolidometer. Further details about the experimental procedure used can be found in
32 Muhammed *et al.* [15].
33
34
35
36
37
38
39
40

41 *Loading protocol*

42 A given test is composed of different successive sequences listed below:

- 43 (i) Installation of the pile-probe at constant displacement rate (1 mm/s) with the long
44 stroke hydraulic jack;
 - 45 (ii) Pre-cyclic static displacement-controlled loading tests up to failure;
 - 46 (iii) Cyclic displacement-controlled sequence;
 - 47 (iv) Post-cyclic static displacement-controlled loading tests up to failure.
- 48
49
50
51
52

53 2.5 - Tested soil

54 The tests presented in this paper have been carried out on saturated specimens of kaolinite
55 Speswhite. The physical properties of this reference clay, as determined by the authors, are
56
57
58
59
60
61
62
63
64
65

1 listed in table 1. The particle size distribution curve of the deflocculated Speswhite clay is
2 shown in Fig. 4.
3
4

5 **3 – PRESENTATION OF A TYPICAL TEST**

6
7

8 A typical test is presented in this section. For this test (Test 1), the initial consolidation of the
9 specimen has been achieved in five steps in the consolidometer, corresponding to successive
10 vertical stresses of 5, 15, 45, 125 and 250 kPa. Then, the pre-consolidated clay specimen has
11 been placed in the calibration chamber and submitted to a final vertical effective stress σ'_{v0} of
12 250 kPa and a final effective horizontal stress σ'_{h0} of 150 kPa corresponding to an estimated
13 value of K_0 equal to 0.59. The permeability and consolidation coefficient of the clay under this
14 state of stress have been determined based on oedometer tests, giving $k = 2.7 \cdot 10^{-9}$ m/s and
15 $c_v = 3.0 \cdot 10^{-7}$ m²/s.
16
17
18
19
20

21 **3.1 - Installation of the pile-probe**

22

23 The probe is initially pushed into the clay specimen with a constant penetration rate of 1 mm/s
24 down to a penetration depth of 460 mm. This depth corresponds to a position of the probe for
25 which the friction sleeve is practically vertically centered in the clay specimen. Measurements
26 of tip resistance, local skin friction and total load head versus probe penetration during the
27 installation sequence are presented in Fig. 5. The tip resistance mobilization is fairly rapid and
28 a plateau is reached after 180 mm of tip penetration. The mobilization of local friction starts
29 when the sleeve friction gets into the soil specimen at about 250 mm of tip penetration after
30 which it increases progressively and reaches an almost stabilized steady state value.
31 This stabilization of tip resistance and local skin friction accounts for a good homogeneity of
32 the clay within the reconstituted specimen, thus validating the specimen preparation protocol.
33 As far as the total head load is concerned, which accounts for the global mobilization of both
34 tip resistance and friction along the probe shaft, a rapid increase is first observed up to 50 mm
35 of the penetration depth. This rapid increase corresponds to the rapid mobilization of tip
36 resistance. Then, a second phase of increase with a lower rate is observed accounting for the
37 progressive increase of the friction surface in the sample.
38

39 During all sequences of a given test, results of tip resistance, local friction and total head load
40 are systematically recovered. This provides fairly good confidence with respect to the measured
41 local values (tip and friction) since at any stage of the test, the values obtained in terms of local
42 friction and tip resistance can be validated by the total head load measurements. However, as
43 mentioned in the objectives of the paper, the focus will mainly be on results concerning local
44 friction in the following.
45
46
47
48
49
50
51
52

53 **3.2 - Pre-cyclic static loading of the probe**

54
55
56

57 The pre-cyclic static (monotonic) loading tests are carried out in order to obtain the failure
58 characteristics in terms of local friction and tip resistance. Two successive displacement-
59 controlled static loadings are performed after full dissipation of the excess pore water generated
60
61
62
63
64
65

1 during pile installation (the probe is left unloaded before static tests for at least 12 hours). The
2 first loading is performed at a displacement rate of 30 $\mu\text{m}/\text{min}$ while the second one is
3 performed at a rate of 300 $\mu\text{m}/\text{min}$ (Fig. 6). A two hours rest was permitted after the first
4 loading.
5

6 A very rapid mobilization of local friction, followed by a plateau, was obtained in both cases
7 (about 34 kPa). Similar results were reported by Mochtar and Edil [13] for a model pile tested
8 in a saturated kaolinitic clay with similar characteristics. It is interesting to note that the results
9 obtained in terms of failure characteristics are very similar for both tests and that the second
10 loading is not significantly affected by the first one. It is also worth mentioning that the local
11 friction mobilized upon initial static tests is almost two times higher than the friction mobilized
12 during installation of the probe. This can be explained by the fact that during the installation
13 phase, very high values of excess pore water pressure (EPWP) can be generated due to full
14 displacement process, which reduces significantly the normal effective stress level acting at the
15 soil-probe interface, resulting in lower values of local friction.
16
17
18
19
20

21 **3.3 - Displacement-controlled cyclic loading**

22
23
24 In order to study the local friction evolution during the application large number of cycles, it is
25 necessary to run displacement-controlled cyclic loading sequences. The key parameters for this
26 type of loading are the displacement amplitude (alternated or non-alternated signal), the signal
27 shape, the frequency of the signal and the number of cycles applied. Fig. 7 presents the results
28 corresponding to Test1, for which 10^5 cycles have been applied. For this typical test, the cyclic
29 displacement amplitude ρ_c was chosen equal to $\pm 250 \mu\text{m}$ (alternated signal) and the shape of
30 the signal is sinusoidal (Fig. 7(a)). The cyclic displacement amplitude chosen gives a high value
31 of ρ_c/ρ_{peak} ratio (ratio between cyclic displacement amplitude and displacement required to
32 mobilize full friction in a static load test). The high value of this ratio allows to better highlight
33 the effect of this parameter on the evolution of local shaft friction during cyclic loading. The
34 test frequency chosen (1 Hz) is intended to study the case of offshore or onshore piles subjected
35 to low speed road traffic or railway traffic (generally varying between 0.1 and 10 Hz).
36
37
38
39
40
41

42 A rapid degradation process is observed from the very first cycle, which keeps going for about
43 40 cycles (Fig. 7(b)). This degradation phase corresponds to cyclic strain-softening of the
44 probe-soil interface. Then, a progressive recovery of mobilized friction is observed (strain-
45 hardening) up to the end of the cyclic sequence with a slight “re-decrease” observed between
46 cycles 300 and 900.
47
48
49

50 A coefficient of friction evolution, called $C_{e,fs}$ (Bekki et al. [2], Muhammed et al. [15]), is
51 introduced to clearly visualize the evolution of local friction mobilization during the application
52 of the cycles. The degradation phases corresponds to a decrease of the value of $C_{e,fs}$ and the
53 reinforcement phases, if there is any, corresponds to an increase of the value of this coefficient.
54
55

$$56 \quad C_{e,fs} = \frac{f_{s,\max(i)} - f_{s,\min(i)}}{f_{s,\max(1)} - f_{s,\min(1)}} \quad (1)$$

57
58
59
60
61
62
63
64
65

1 where $f_{s,\max(1)}$ and $f_{s,\max(i)}$ are the maximum skin friction measured on first cycle and cycle i
2 respectively (push-in phases), $f_{s,\min(1)}$ and $f_{s,\min(i)}$ being the values of minimum skin friction
3 measured on first cycle and on cycle i respectively (pull-out phases).
4
5
6

7 Fig. 8 shows the evolution of C_{efs} versus number of cycles. Most of the degradation occurs
8 within the first 40 cycles. The minimum value reached is about 0.44 which is a low value
9 corresponding to a significant degradation level due to the large cyclic displacement amplitude
10 selected. After the degradation phase, the reinforcement phase toward the end of the cyclic
11 sequence can be observed with a slight decrease between cycle n° 300 to cycle n° 900.
12 Muhammed et al. [15] have explained the behavior observed during the application of the cycles
13 in terms of the evolution of the effective normal stress acting on the probe shaft, σ'_n . The local
14 friction mobilized being equal to $f_s = \sigma'_n \text{tg } \delta_{mob}$, δ_{mob} being the mobilized friction coefficient. It
15 is well known that the evolution of effective normal stress depends on the evolution of excess
16 pore water pressure (EPWP). Any variation of the EPWP results in a variation of effective
17 normal stress.
18
19
20
21
22
23

24 Since the tested soil is a kaolinite, characterized by a rather low permeability, one can expect
25 that the applied cyclic shear at 1 Hz frequency will result in the development of EPWP close to
26 the soil-probe interface. A heterogeneous field of EPWP will be created within a small thickness
27 annulus around the probe, resulting in high hydraulic gradients and initiation of EPWP
28 dissipation. Since the interface shearing is not fully undrained, the problem is therefore coupled
29 with combination of EPWP generation and dissipation. There is, indeed, a competition between
30 the excess pore water pressure generation mechanism due to “undrained” cyclic deformation of
31 the clay around the sleeve, and the EPWP dissipation, which starts taking place from the very
32 beginning of the cyclic sequence due to the radial hydraulic gradient created by the excess pore
33 pressure field. During the initial phase of the sequence (small numbers of cycles), the generation
34 mechanism should be predominant with respect to dissipation, which should result in a
35 relatively rapid increase of EPWP, a corresponding decrease in the normal effective stress and
36 corresponding decrease of mobilized friction (cyclic strain-softening). Then, the dissipation
37 process should become predominant, resulting in a progressive decrease of the EPWP, re-
38 increase of σ'_n and corresponding re-increase of mobilized friction (cyclic strain-hardening).
39 This hypothesis is in full agreement with the results published by Procteur and Khaffaf [21] and
40 Muhammed *et al.* [15].
41
42
43
44
45
46
47
48

49 **3.4 - Final phase of static loading**

50
51 The influence of the cyclic sequence on the post-cyclic static response of the interface has been
52 investigated by performing two post-cyclic static loading tests. The two post-cyclic static tests
53 were performed at the same displacement rate of 300 $\mu\text{m}/\text{min}$ up to failure (4 mm of vertical
54 displacement). The first post-cyclic static test was performed directly after the end of the cyclic
55 sequence. The second post-cyclic static test was performed after a resting period of two hours
56 after the first test, allowing pore water pressure equilibrium of the soil around the probe. Fig. 9
57
58
59
60
61
62
63
64
65

1 shows the evolution of mobilized local friction versus vertical displacement for the two
2 successive post-cyclic static tests. A significant difference may be observed between the two
3 loadings tests. For the first test, a sharp peak of friction (of about 54 kPa) is obtained for a tip
4 displacement of about 500 μm , followed by a rapid strain softening and a stabilization at an
5 ultimate value of about 25 kPa. For the second test, the response observed is qualitatively very
6 similar to the response observed for the pre-cyclic static tests. No peak is observed and full
7 mobilization of friction is obtained for a very small displacement (about 100 μm) followed by
8 a constant friction plateau of about 23 kPa. It is worth noting that the ultimate value of friction
9 obtained at large displacements is very similar for both loadings.

10
11 In order to quantify the influence of the cycles on the post-cyclic static response, the degradation
12 factor of skin friction, D_τ as defined by Poulos [20], has been used:

$$13 \quad D_\tau = \frac{\text{property after cyclic loading}}{\text{property for initial static loading}} \quad (2)$$

14
15 It is interesting to note that the value obtained for D_τ factor ($D_\tau=0.70$) is fairly close to the
16 value obtained for the coefficient of evolution $C_{e,fs}$ ($C_{e,fs}=0.72$) at the end of the cyclic sequence
17 (cycle n° 10⁵) accounting for a good consistency between the two coefficients.

18 19 20 21 22 23 24 25 26 27 28 29 30 31 **4 – INFLUENCE OF CYCLIC DISPLACEMENT AMPLITUDE AND INITIAL** 32 **STATE OF SPECIMEN ON LOCAL FRICTION EVOLUTION**

33
34 In order to evaluate the influence of cyclic displacement amplitude and initial state of specimen
35 in terms of initial state of stress on the mobilization of local friction, a series of five tests has
36 been carried out. All specimens were normally consolidated and were saturated with no
37 application of backpressure. Table 2 summarizes the main characteristics of the tests carried
38 out.

39 40 41 42 43 **4.1 - Influence of the cyclic displacement amplitude**

44
45 A very important parameter involved in the evolution of local friction upon cyclic tests is the
46 cyclic displacement amplitude, ρ_c , which controls the evolution of interface properties. Real
47 piles are generally head-loaded in a force-controlled way (either monotonic or cyclic loading).
48 However, locally, along the shaft and under cyclic loading, this head loading results, at a given
49 depth along the pile shaft, in a cyclic displacement with a given amplitude during a certain
50 number of cycles, controlling the interface properties evolution. The cyclic displacement
51 amplitude is not the same at all depths along the pile shaft (usually larger toward the pile head
52 and smaller toward the pile toe) depending on the rigidity of the pile and the head loading
53 amplitude. The calibration chamber setup, allowing to run displacement-controlled loadings, is
54 therefore an appropriate tool to quantify the influence of this parameter on the evolution of local
55 interface frictional properties.

1 Three tests, Test 1, Test 2 and Test 3 (table 1), have been performed under the same initial state
2 of stress applied to the specimen. These tests were intended to quantify the influence of the
3 cyclic displacement amplitude on the evolution of mobilized local friction upon cyclic loading
4 and subsequent post-cyclic static friction. The vertical and horizontal stresses applied to the
5 specimen, the number of cycles and the loading frequency were kept constant while the cyclic
6 displacement amplitude was varied from low to high values. Before presenting the behavior
7 observed upon cyclic sequences, Fig. 10 shows the repeatability of the measurements upon pre-
8 cyclic static tests for the three tests, indicating a good consistency between the results (with a
9 maximum variance of 10% at failure).
10

11 The influence of the cyclic displacement amplitude on the evolution of skin friction upon cyclic
12 loading is shown in Fig. 11 in terms of the coefficient of evolution. Three cyclic displacement
13 amplitudes, i.e., $\pm 100 \mu\text{m}$, $\pm 250 \mu\text{m}$ and $\pm 500 \mu\text{m}$, have been applied for Test 2, Test 1 and
14 Test 3, respectively. These values of cyclic displacement amplitude represent low to high ratios
15 of ρ_c/ρ_{peak} (ratio between cyclic displacement amplitude, applied during the cyclic sequence,
16 and displacement required to mobilize full friction in a static load test). This Figure clearly
17 shows that the skin friction degradation rate increases with increasing cyclic displacement
18 amplitude. This increase of the degradation rate could be explained in terms of EPWP
19 generation around the probe. In fact, higher values of cyclic displacement amplitude induces
20 relatively higher values of EPWP resulting in higher decrease in the effective normal stress and
21 corresponding higher decrease of mobilized friction (cyclic strain-softening). For high to very
22 high values of applied cyclic displacement amplitudes, after the degradation phase, a
23 progressive phase of reinforcement can be observed. This reinforcement phase can be attributed
24 to the EPWP dissipation. In fact, for high values of cyclic displacement amplitude, the induced
25 high values of EPWP around the sleeve will first increase rapidly and then decrease after
26 passing through a maximum value due to the dissipation phenomena, which becomes
27 predominant rapidly.
28

29 After the cyclic sequence, two post cyclic static tests has been performed for each specimen at
30 a displacement rate of $300 \mu\text{m}/\text{min}$ (same loading procedure as for the typical test). The
31 influence of the cyclic displacement amplitude on the evolution of skin friction upon post-cyclic
32 static loading is presented in Fig. 12. Qualitatively, results are similar. For the three tests,
33 a sharp peak of skin friction is obtained upon the first post-cyclic static loading followed by
34 significant strain softening which keeps going with progressive stabilization for large
35 displacements. However, quantitatively, a clear distinction of the post cyclic behavior can be
36 observed for different cyclic displacement amplitudes tested. The test results show that the peak
37 value of skin friction, obtained upon the first post-cyclic static test, increases with increasing
38 the cyclic displacement amplitude applied during the cyclic loading. For the lowest cyclic
39 displacement amplitude ($\pm 100 \mu\text{m}$), the corresponding peak value is 43 kPa reached at 0.25mm
40 of probe displacement. This value of local friction is fairly close the one mobilized upon pre-
41 cyclic static tests while for the highest cyclic displacement amplitude ($\pm 500 \mu\text{m}$), the
42 corresponding peak value is 70 kPa reached after 0.95mm of probe displacement. It is
43 interesting to note that the required displacement to reach the full mobilization of local friction
44 (peak of local friction), upon post-cyclic static tests, also increases with increasing the cyclic
45 displacement amplitude (Fig. 13).
46
47
48
49
50
51
52
53
54
55
56
57
58
59
60
61
62
63
64
65

1 One may attribute the variation in the values of the peak and required displacement to reach the
2 peak, to the induced thickness of the modified zone around the probe after cyclic loading. The
3 authors believe that higher cyclic displacement amplitude influences larger zone within the soil
4 around the probe, thus resulting in a thicker modified interface zone. The soil within this zone,
5 characterized as the modified zone of interface, undergoes shearing and variation of EPWP
6 during the cyclic loading (coupled generation and dissipation phases). Recently,
7 Muhammed *et al.* [17] showed that the soil within this zone presents a very different type of
8 response upon post-cyclic static tests with respect to the one observed for the initial pre-cyclic
9 static loadings. These authors have observed a significant decrease of the measured PWP
10 (generation of negative excess pore water pressure EPWP) at the clay-probe interface upon
11 post-cyclic static tests accounting for the modification of the soil-probe interface properties
12 after cyclic loading. The authors have also indicated that this negative EPWP corresponds to a
13 dilative behavior representative of an overconsolidated state of the clay at the soil-probe
14 interface due to the cyclic loading. Thus, after the cyclic loading, the thicker overconsolidated
15 modified zone around the probe presents higher values of friction and requires necessarily more
16 displacement to be sheared upon post-cyclic static test, as shown on the 2D conceptual scheme
17 presented in Fig. 14.

18 In terms of friction degradation at the end of each loading stage, i.e. end of cyclic and post-
19 cyclic static loadings, results show close values between the coefficient of evolution, $C_{e,fs}$, at
20 the end of cyclic loading and degradation factor of skin friction obtained from static tests, D_τ ,
21 which is consistent and gives more confidence to the results obtained.

22 **4.2 - Influence of the initial state of effective stress applied to the specimen**

23 Another parameter that can be investigated in calibration chamber is initial state of effective
24 stress applied to the specimen. This parameter is representative of a given depth within the soil
25 below the ground surface: the higher the effective state of stress and the deeper the soil element.
26 In calibration chamber, the effect of this parameter can be investigated by changing the values
27 of horizontal and vertical confining pressure applied to the specimen. This allows to study the
28 behavior of a pile segment at any depth.

29 Results of three tests, Test 1, Test 4 and Test 5 (Table 1), with three different initial states of
30 stress, have been compared, corresponding to the state of a pile segment at three different depths
31 below the ground surface.

32 The same loading procedure as the one described in the typical test was implemented here again
33 for successive loading sequences: installation phase, pre-cyclic static phases, cyclic sequence
34 and for post-cyclic static phases. The influence of the initial state of effective stress on the
35 evolution of local friction versus probe penetration during the installation and subsequent pre-
36 cyclic static tests is presented in Fig. 15. For the three stress levels tested, the mobilized skin
37 friction and initial stiffness increase linearly with increasing the applied effective state of stress,
38 which is consistent. It is important to notice that, upon initial static tests, the required
39 displacement to mobilize full local friction increases with increasing the effective consolidation
40 stress level.

The influence of the initial state of stress on the evolution of skin friction upon cyclic loading is shown in Fig. 16. The cyclic displacement amplitude, the number of cycles and the loading frequency were the same for the three tests. Again, the comparison is made in terms of coefficient of evolution. This figure shows that the rate of local friction degradation decreases with the increase in the initial effective stress. This can be explained in terms of the ρ_c/ρ_{peak} ratio, which dominates the amount of degradation of the interface (Poulos [20]). The higher the value of ρ_c/ρ_{peak} ratio and the higher the degradation rate. For the three cyclic tests presented here, the ρ_{peak} value increases with increasing initial effective state of stress (visible in Fig. 15b) resulting in lower values of ρ_c/ρ_{peak} ratio and corresponding smaller rates of friction degradation.

As far as the post-cyclic static responses are concerned, results show that the mobilized local friction (maximum value $f_{s,peak}$ and ultimate value $f_{s,lim}$) increases with increasing initial effective state of stress. However, the required displacement to mobilize full local friction after the cyclic sequence decreases with increasing initial effective state of stress. This could be explained, again, in term of thickness of the modified zone created after cyclic loading. Since upon cyclic loading, higher initial effective state of stress allows lower degradation. It is thus believed that, thinner modified interface zone is formed for higher levels of applied effective stress after the cyclic loading. This means that the modified interface zone created for low consolidation stress level ($\sigma'_{v0}= 125$ kPa - $\sigma'_{h0}= 72$ kPa) is thicker than the ones formed for medium ($\sigma'_{v0}= 250$ kPa - $\sigma'_{h0}= 150$ kPa) and high ($\sigma'_{v0}= 420$ kPa - $\sigma'_{h0}= 252$ kPa) consolidation stress level, requiring necessarily more displacement to be sheared upon post-cyclic static test. It is also instructive to estimate the degradation factor of skin friction from Fig. 17. The specimen with the higher initial state of stress corresponds to higher D_τ factor value corresponding to lower amount of degradation. The estimated values of D_τ factor are 0.58, 0.70 and 0.88 for ($\sigma'_{v0}= 125$ kPa - $\sigma'_{h0}=72$ kPa), ($\sigma'_{v0}= 250$ kPa - $\sigma'_{h0}=150$ kPa) and ($\sigma'_{v0}= 420$ kPa - $\sigma'_{h0}=252$ kPa) respectively. It is interesting to note that there is a reasonable agreement between the degradation factor values and the coefficient of evolution values at the end of cyclic loading.

5 –SYNTHESIS OF THE RESULTS

To better analyze the effect of cyclic displacement amplitude and initial state of stress applied to the specimen, on the local interface friction, the results of the present work are synthesized in this section. Concerning the local friction mobilization upon displacement-controlled static tests, Fig. 18 shows the evolution of maximum and ultimate values reached in terms of local friction upon static tests. In the same figure, a comparison is made with the maximum value of friction mobilized upon installation phase. Results clearly show a quasi-linear relationship between the local friction and initial state of effective stress (Fig. 18a and 18b). The higher the initial state of effective stress and the higher the values of mobilized local friction. Fig. 18a and 18b also emphasize that the mobilized local friction upon installation phase is much smaller than the one mobilized upon initial static loadings (nearly half). This aspect has been explained by the fact that during installation phase, high local values of excess pore water pressure is

1 generated due to the high increase of total stresses during the deep penetration process as the
2 soil is forced outwards to accommodate the volume of the probe. This, decreases the effective
3 normal stress acting on the pile shaft and by consequent, the mobilized friction reduces. During
4 static loadings, the applied displacement rate is significantly smaller and the corresponding
5 EPWP generation within the soil is limited to a thin layer around the probe. The corresponding
6 mobilization is then higher. This interpretation is in reasonable agreement with the results
7 published by Randolph [22], Gavin and Gallagher [5], O'Beirne [18] and Hosseini and
8 Rayhani [7] and Muhammed *et al.* [17].

9
10 As far as the effect of cyclic loading parameters on the evolution of local friction is concerned,
11 in Fig. 19, the relationship between the coefficient of evolution and the degradation factor with
12 the applied cyclic displacement amplitude and the initial consolidation level is synthetized.
13

14 This figure has an important practical implication as it demonstrates clearly the effect of both
15 parameters on the degradation of local skin friction. Fig. 19a synthetizes the effect of cyclic
16 displacement amplitude on the evolution of the degradation factor and of the coefficient of
17 evolution. The figure shows clearly that the minimum value of $C_{e,fs}$, corresponding to maximum
18 degradation, decreases with the increase in the applied cyclic displacement amplitude, which is
19 consistent and has been explained in terms of EPWP generation around the probe. The values
20 of $C_{e,fs}$ at the end of the cyclic tests, i.e. cycle number 10^5 , are fairly close for the three cyclic
21 displacement amplitudes after converging towards a completely drained regime with full
22 dissipation of EPWP and corresponding re-increase of effective normal stress. The values of
23 $C_{e,fs}$ at the end of the cyclic tests are confirmed by the values of degradation factor D_τ .

24
25 Fig. 19b synthetizes the effect of initial state of effective stress on the evolution of the
26 degradation factor and the coefficient of evolution. This figure shows clearly that the minimum
27 value of $C_{e,fs}$, corresponding to maximum degradation, increases with the increase in effective
28 horizontal stress. This aspect has been explained in terms of the thickness of the influenced
29 zone created by the cyclic loading, which should be smaller for higher effective horizontal
30 stress. The values of $C_{e,fs}$ at the end of the cyclic tests, i.e. cycle number 10^5 , and D_τ also increase
31 with the increase of effective horizontal stress thus confirming the above interpretations made.
32 Finally, Table 3 gives a brief synthesis of the results in terms of the coefficient of evolution and
33 degradation factor. A reasonable degree of consistency in the results can be observed.
34
35
36
37
38
39
40
41
42
43
44

45 6 – CONCLUSIONS

46
47 Evolution of local friction mobilisation during static and cyclic axial loadings at various initial
48 state of stress and at different cyclic displacement amplitude was investigated. The experiment
49 is based on the use of an instrumented pile-probe installed and loaded in specimens of saturated
50 clay reconstituted in a calibration chamber. The following conclusions can be drawn:
51
52

- 53 • The local friction mobilized upon installation phase is much smaller than the one
54 mobilized upon initial static loadings.
- 55 • The local friction and displacement required to mobilize full friction in a static test
56 increase with increasing the initial state of effective stress applied to the specimen.
57
58
59
60
61
62
63
64
65

- The cyclic degradation of local friction is mainly controlled by the cyclic displacement amplitude applied. For the same initial state of the specimen, number of cycles and cyclic frequency, the skin friction degradation is higher for higher values of cyclic displacement amplitude.
- The cyclic displacement amplitude causing major friction degradation can be directly related to the displacement required to mobilize full local friction in a static test.
- For the same cyclic displacement amplitude, number of cycles and frequency, the skin friction degradation is smaller for higher values of initial consolidation pressure.

REFERENCES

1. Al-Douri R H, Poulos H G (1995) Predicted and Observed Cyclic Performance of Piles in calcareous sand. *Journal of Geotechnical Engineering, ASCE*, 121 (1): 1-16.
2. Bekki H, Canou J, Tali B, Dupla J-C, Bouafia A (2013) Evolution of Local Friction Along a Model Pile Shaft in a Calibration Chamber for a Large Number of Loading Cycles. *Comptes Rendus – Mecanique*, 341(6): 499-507.
3. Chan S F, Hanna T H (1980) Repeated Loading on Single Piles in Sand. *Journal of Geotechnical Engineering*, 106(2): 171-188.
4. Chin J T, Poulos H G (1996) Tests on Model Jacked Piles in Calcareous Sand. *Geotechnical Testing Journal*, 19(2): 164-180.
5. Gavin K, Gallagher D (2005) Development of Shaft Friction on Driven Piles in Sand and Clay. Paper Presented to Engineers Ireland, 10th October 2005. *Trans IEI 2005*. (Geotechnical Prize Paper). Published on www.ei.ie in October 2005
6. Goulois A, Whitman R V, Høeg K (1985) Effects of Sustained Shear Stresses on the Cyclic Degradation of Clay. *Strength Testing of Marine Sediments: Laboratory and In-situ Measurements*. ASTM STP 883, R. C. Chaney and K. R. Demars, Eds., American Society for testing and Materials, Philadelphia: 336-351.

- 1
2
3
4
5
6
7
8
9
10
11
12
13
14
15
16
17
18
19
20
21
22
23
24
25
26
27
28
29
30
31
32
33
34
35
36
37
38
39
40
41
42
43
44
45
46
47
48
49
50
51
52
53
54
55
56
57
58
59
60
61
62
63
64
65
7. Hosseini M A, Rayhani M (2017) Evolution of pile shaft capacity over time in marine soils. International Journal of Geo-Engineering, 8(1), 12. <http://doi.org/10.1186/s40703-017-0049-8>.
8. Le Kouby A, Canou J, Dupla J-C (2004) Behaviour of Model Piles Subjected to Cyclic Axial Loading. In Proceedings of the International Conference on Cyclic Behaviour of Soils and Liquefaction Phenomena, Bochum, Germany, 31 March - 2 April 2004, pp 159-166.
9. Lee C Y, Poulos H G (1990) Experimental Investigations of Axial Capacity of Model Grouted Piles in Marine Calcareous Sediments. Research Report No. R618, University of Sydney, School of Civil and Mining Engineering.
10. Lee C Y, Poulos H G (1993) Cyclic analysis of axially loaded piles in calcareous soils. Canadian Geotechnical Journal, 1993, 30(1): 82-95, <https://doi.org/10.1139/t93-008>
11. Lehane B M, White D J (2004) Friction Fatigue on Displacement Piles in Sand. Géotechnique, 54(10): 645-658.
12. Matlock H, Bogard D, Cheang L (1982) A Laboratory Study of Axially Loaded Piles and Pile Groups Including Pore Pressure Measurements. In Proceeding of The Third International Conference on the Behavior of Offshore Structure (BOSS), Vol. 1, pp 105-121.
13. Mochtar I B, Edil T B (1988) Shaft resistance of model pile in clay. Journal of Geotechnical Engineering, 114(11): 1227-1244
14. Muhammed R D (2015) Etude en Chambre d'étalonnage du Frottement Sol-Pieu sous Grands Nombres de Cycles. Application au Calcul des Fondations Profondes dans les Sols Fins Saturés. Doctoral thesis. Université Pierre et Marie Curie - Paris VI, 219 p.

- 1
2
3
4
5
6
7
8
9
10
11
12
13
14
15
16
17
18
19
20
21
22
23
24
25
26
27
28
29
30
31
32
33
34
35
36
37
38
39
40
41
42
43
44
45
46
47
48
49
50
51
52
53
54
55
56
57
58
59
60
61
62
63
64
65
15. Muhammed R D, Canou J, Dupla J-C, Tabbagh A (2018a) Evaluation of local soil-pile friction in saturated clays under cyclic loading. *Soils and Foundations*. <https://doi.org/10.1016/j.sandf.2018.06.006>
 16. Muhammed R D, Canou J, Dupla J-C, Tabbagh A (2018b) Laboratory Study of Local Clay-Pile Friction Evolution for Large Numbers of Cycles. In: Tran-Nguyen HH., Wong H., Ragueneau F., Ha-Minh C. (eds) *Proceedings of the 4th Congrès International de Géotechnique - Ouvrages -Structures*. CIGOS 2017. *Lecture Notes in Civil Engineering*, vol 8. Springer, Singapore, https://doi.org/10.1007/978-981-10-6713-6_74
 17. Muhammed R D, Canou J, Dupla J-C, Tabbagh A (2019) Evaluation of local friction and pore water pressure evolution along instrumented probes in saturated clay for large numbers of cycles. *Canadian Geotechnical Journal*. (accepted with minor revisions)
 18. O'Beirne C P (2016) Development of design approaches for dynamically installed anchors validated through field and centrifuge studies. Doctoral Thesis, The University of Western Australia.
 19. Poulos H G (1981). Some Aspects of Skin Friction of Piles in Clay Under Cyclic Loading. *Geotechnical Engineering*, 12(1), pp 1-17.
 20. Poulos H G (1982) Influence of Cyclic Loading on Axial Pile Response. R413 Monograph, University of Sydney, Sydney, New South Wales 2006 Australia, 36 p.
 21. Procter D C, Khaffaf J H (1987) Cyclic axial displacement tests on model piles in clay. *Géotechnique* 37(4): 505-509.
 22. Randolph M F (2003) Science and empiricism in pile foundation design. *Geotechnique*, 53(10), pp 847–875.

23. Tsuha C H C, Foray P Y, Jardine R J, Yang Z X, Silva M, Rimoy S (2012) Behaviour
of Displacement Piles in Sand Under Cyclic Axial Loading. *Soils and Foundations*,
52(3): 393-410.

1
2
3
4
5
6
7
8
9
10
11
12
13
14
15
16
17
18
19
20
21
22
23
24
25
26
27
28
29
30
31
32
33
34
35
36
37
38
39
40
41
42
43
44
45
46
47
48
49
50
51
52
53
54
55
56
57
58
59
60
61
62
63
64
65

Evolution of cyclic local friction along clay-pile interface for very large numbers of cycles: parametric study

Figures

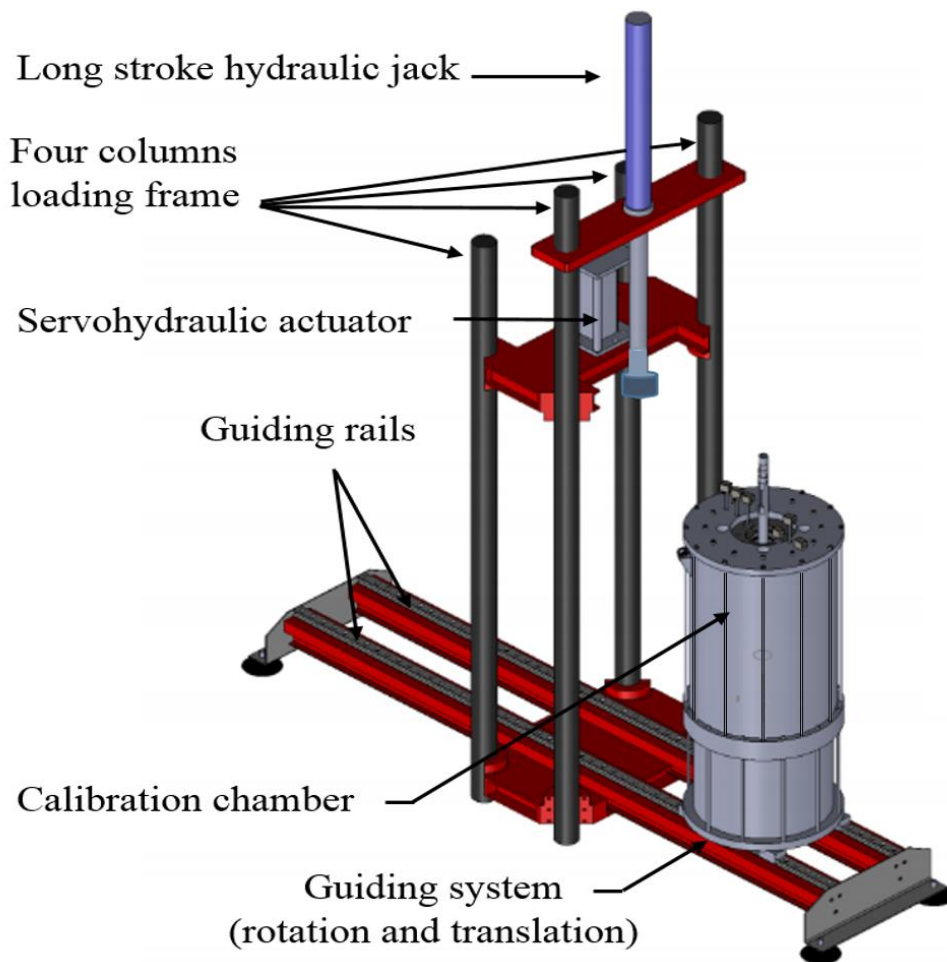


Fig. 1. General 3D view of the experimental setup

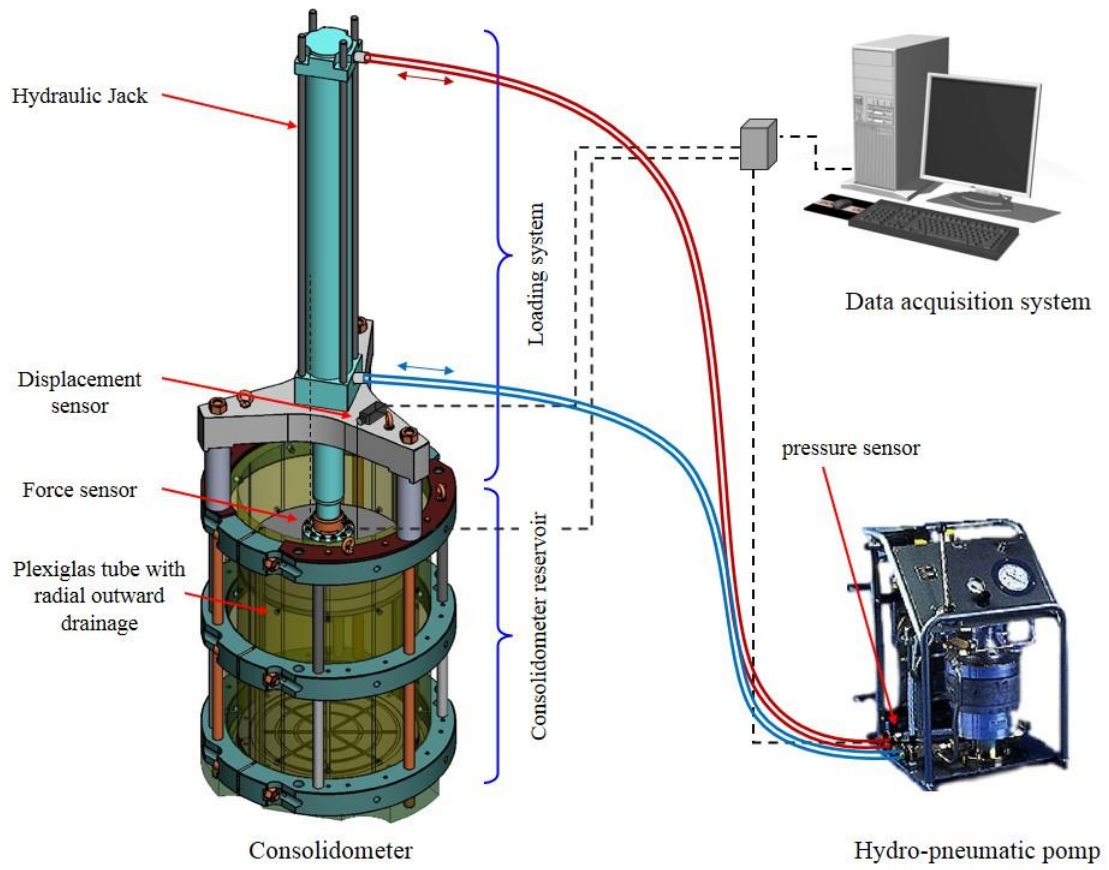


Fig. 2. General view of the consolidometer set up and ancillary equipment

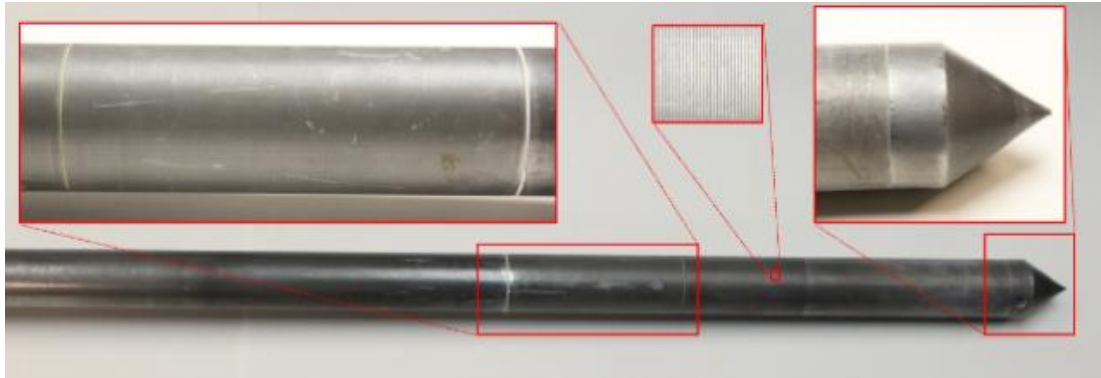
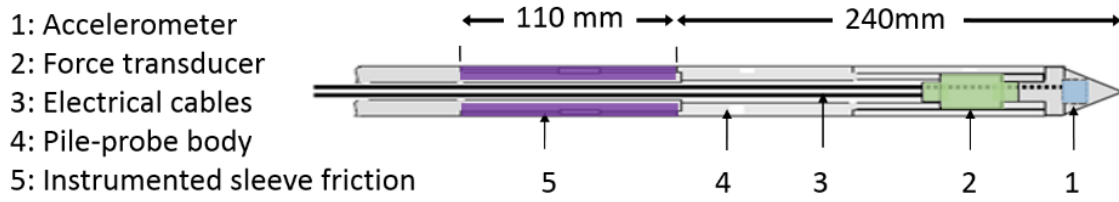


Fig. 3. Simplified cross-section and view of the instrumented pile-probe

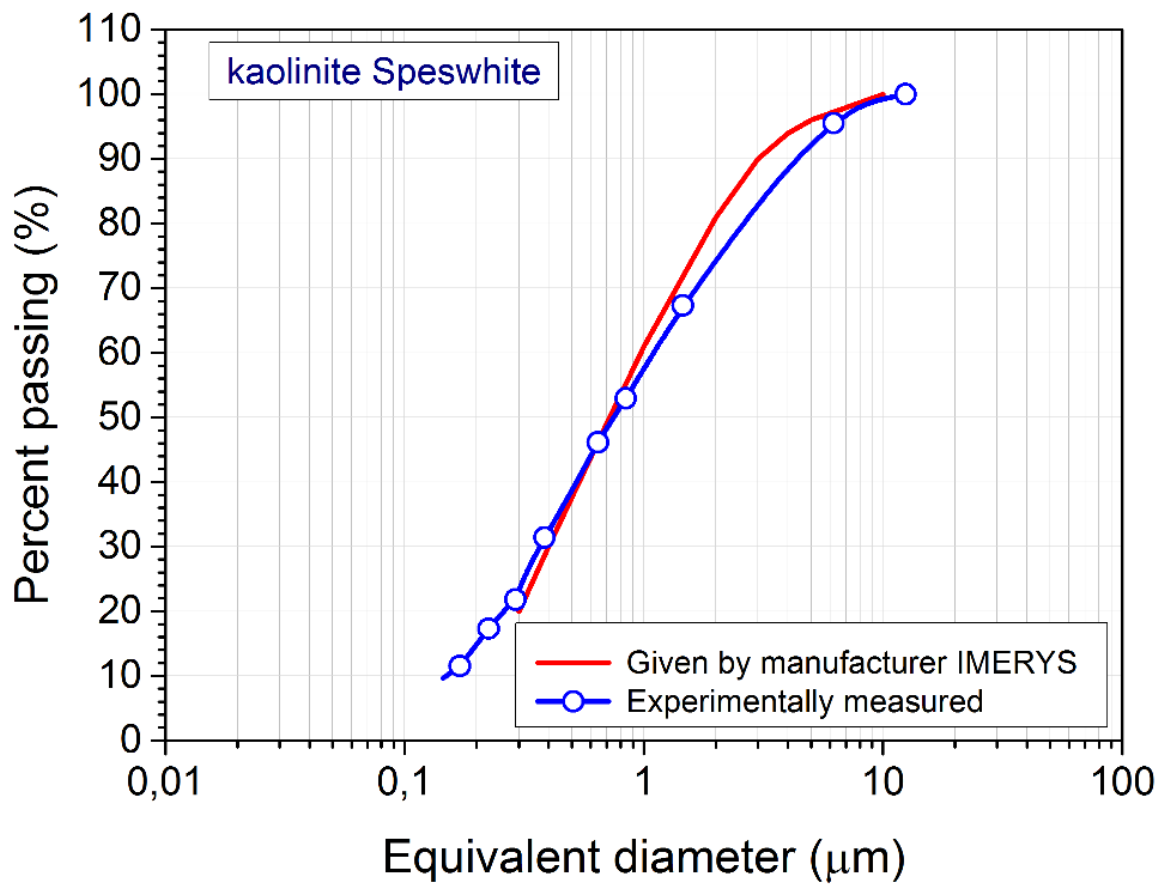


Fig. 4. Particle size distribution of Speswhite

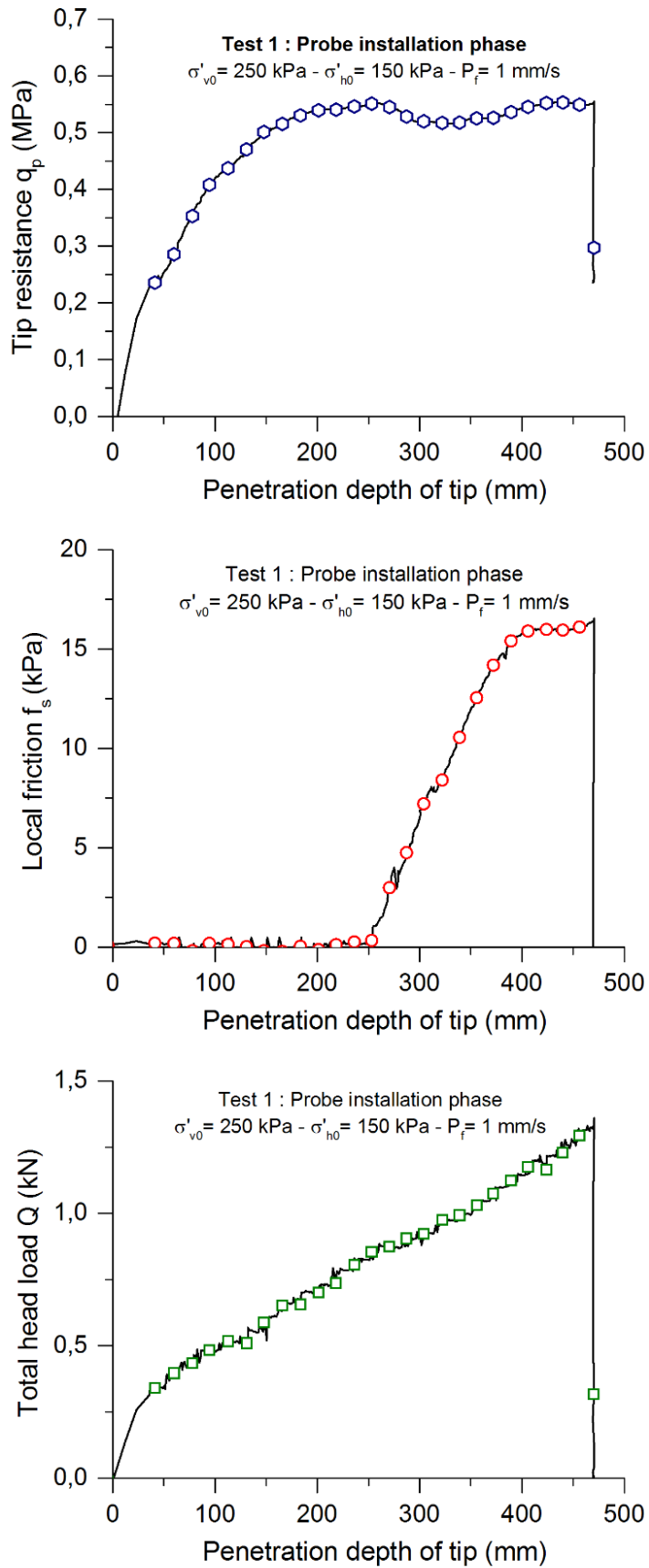


Fig. 5. Installation phase: (a) tip resistance versus penetration depth; (b) local friction versus penetration depth; (c) total load applied versus penetration depth

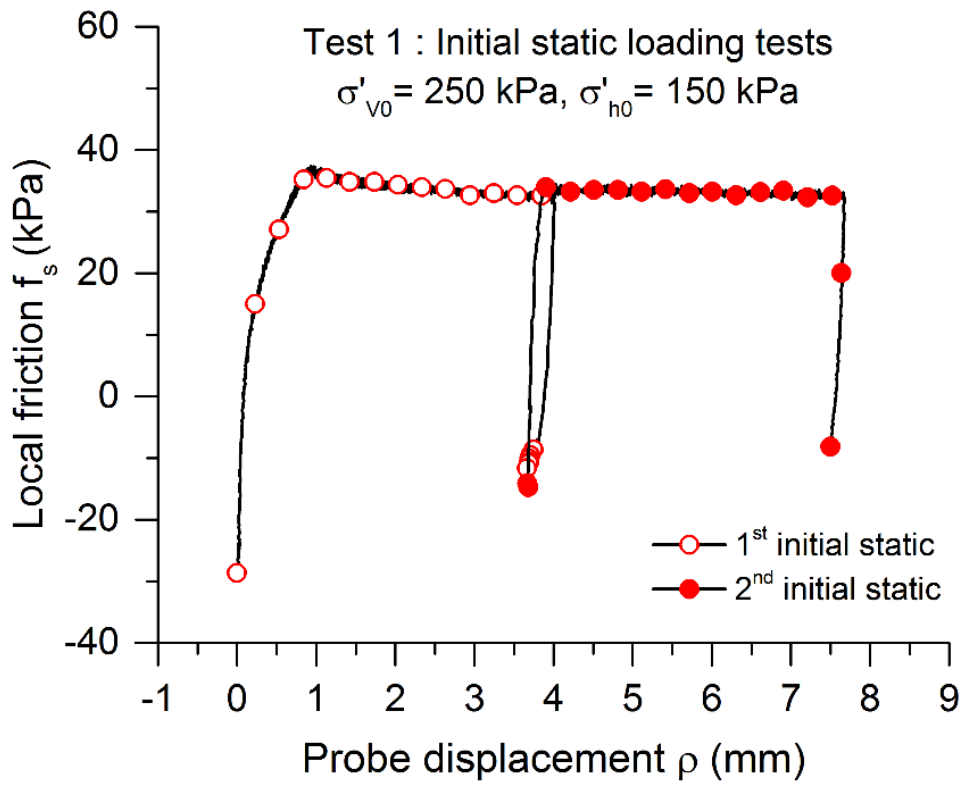


Fig. 6. Initial static loading tests: (a) tip resistance versus vertical displacement; (b) local friction versus vertical displacement; (c) total load applied versus vertical displacement

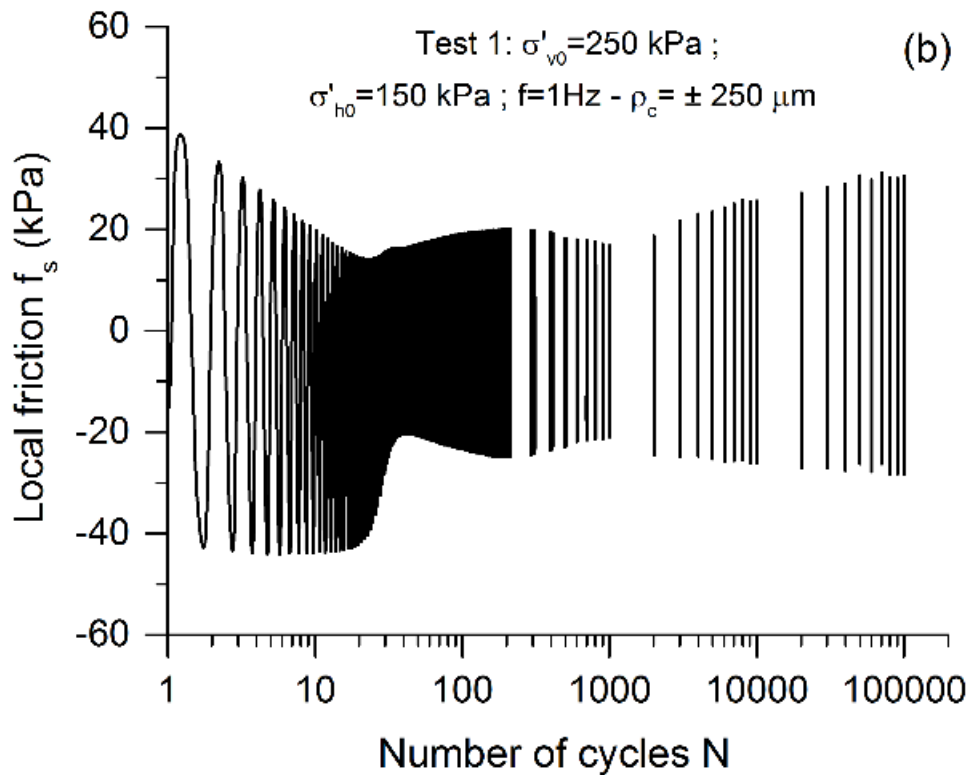
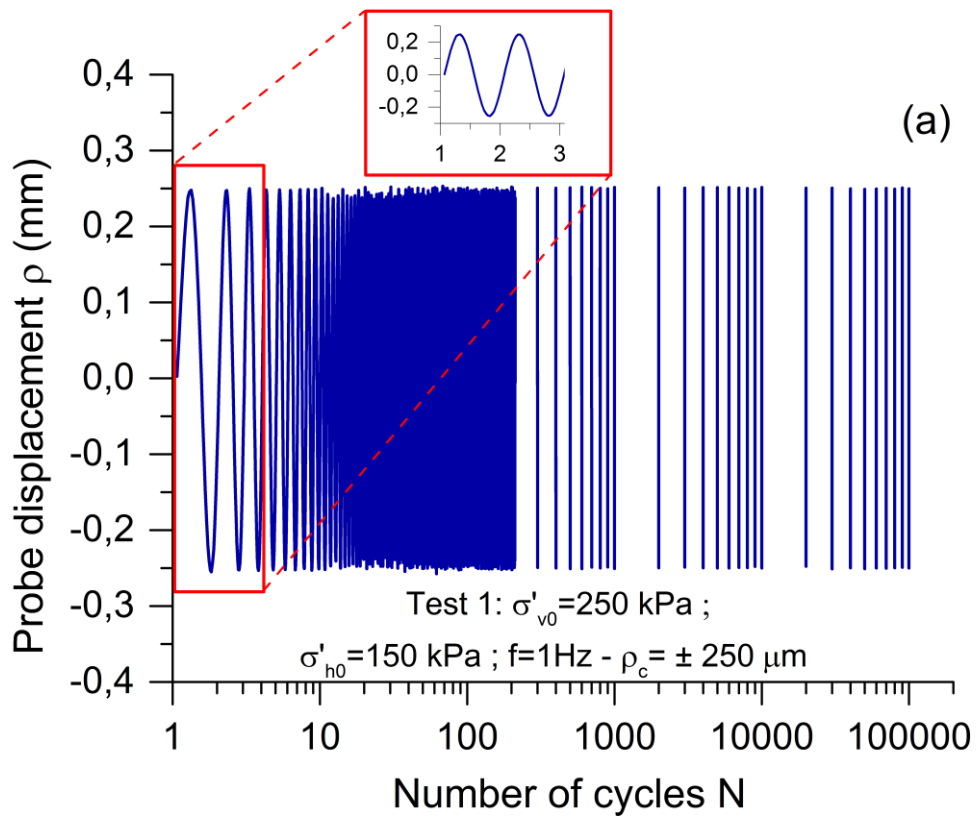


Fig. 7. Cyclic loading phase: (a) displacement-controlled loading signal versus number of cycles; (b) local friction versus number of cycles

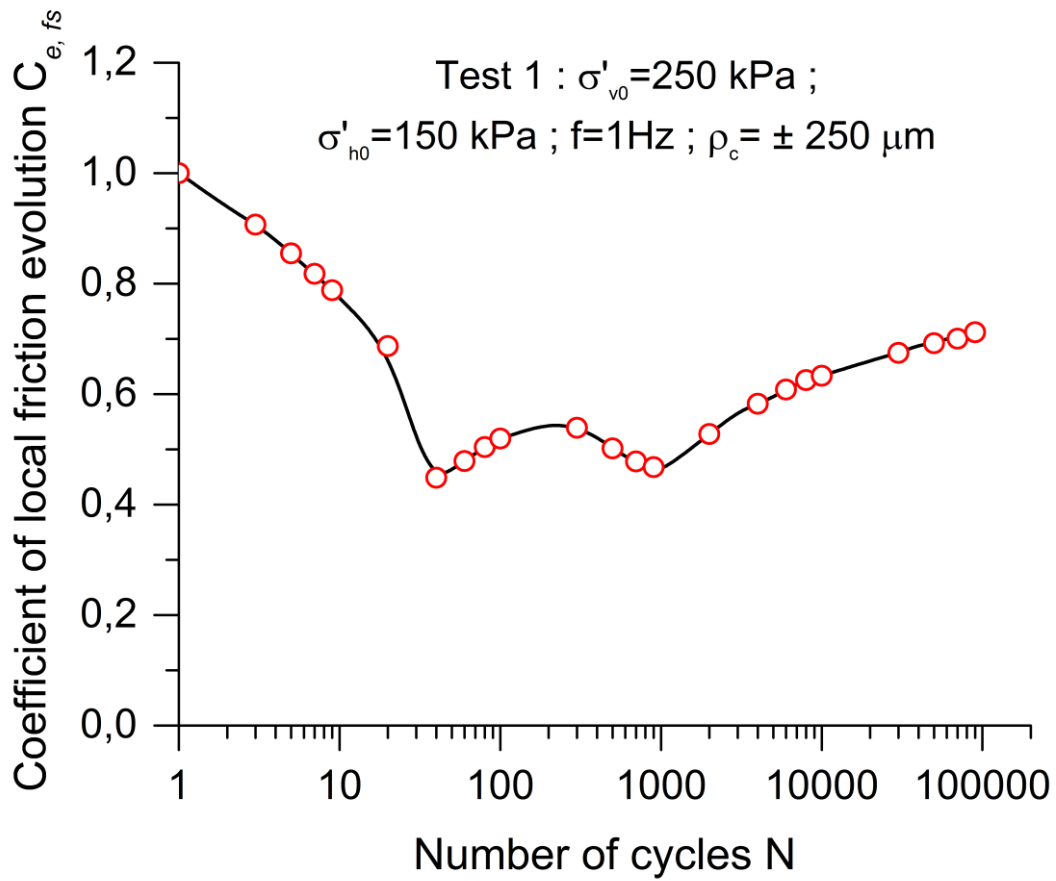


Fig. 8. Cyclic sequence: Coefficient of evolution ($C_{e,fs}$) versus number of cycles

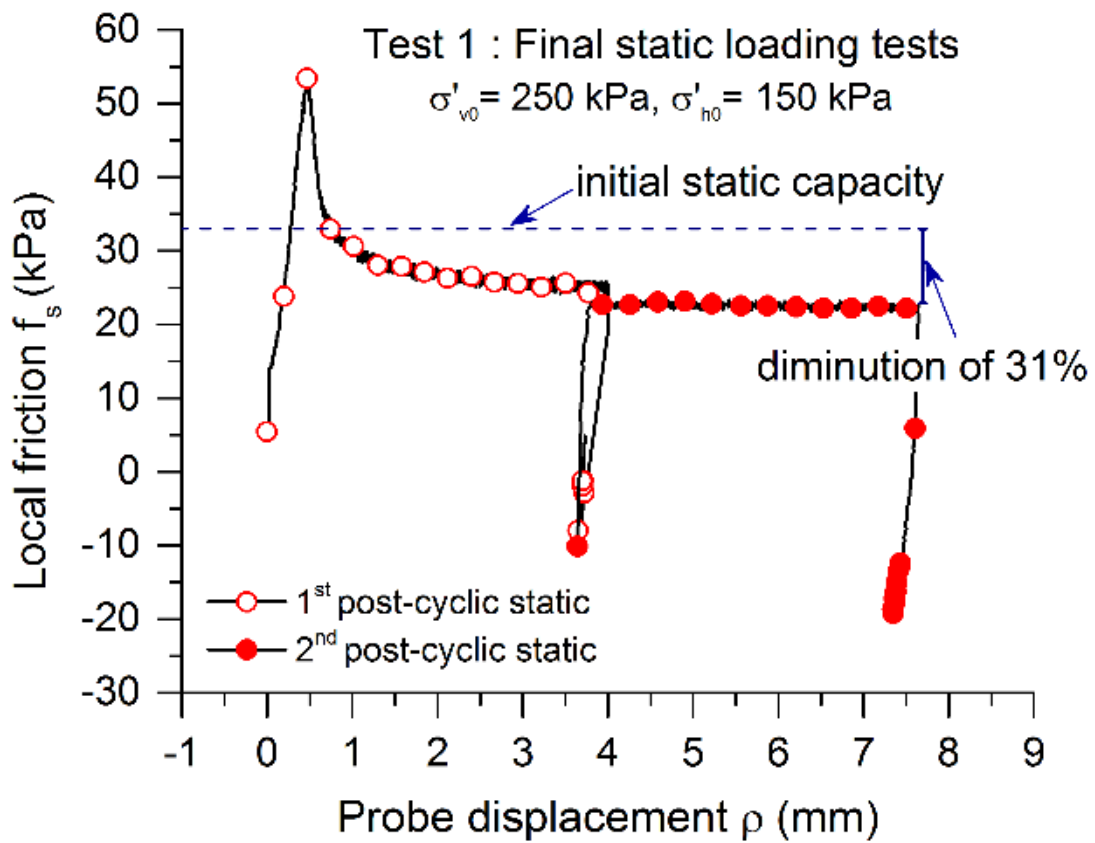


Fig. 9. Final static loading phase: (a) tip resistance versus vertical displacement; (b) local friction versus vertical displacement

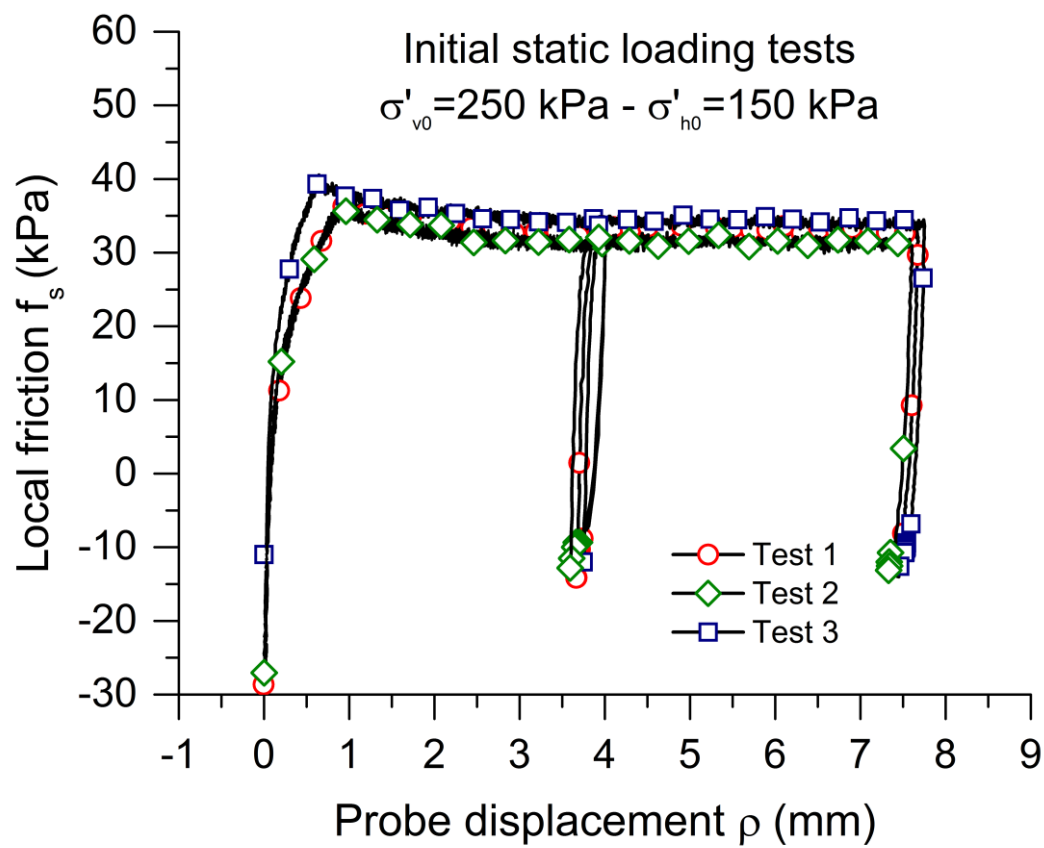


Fig. 10. Repeatability of pre-cyclic static tests

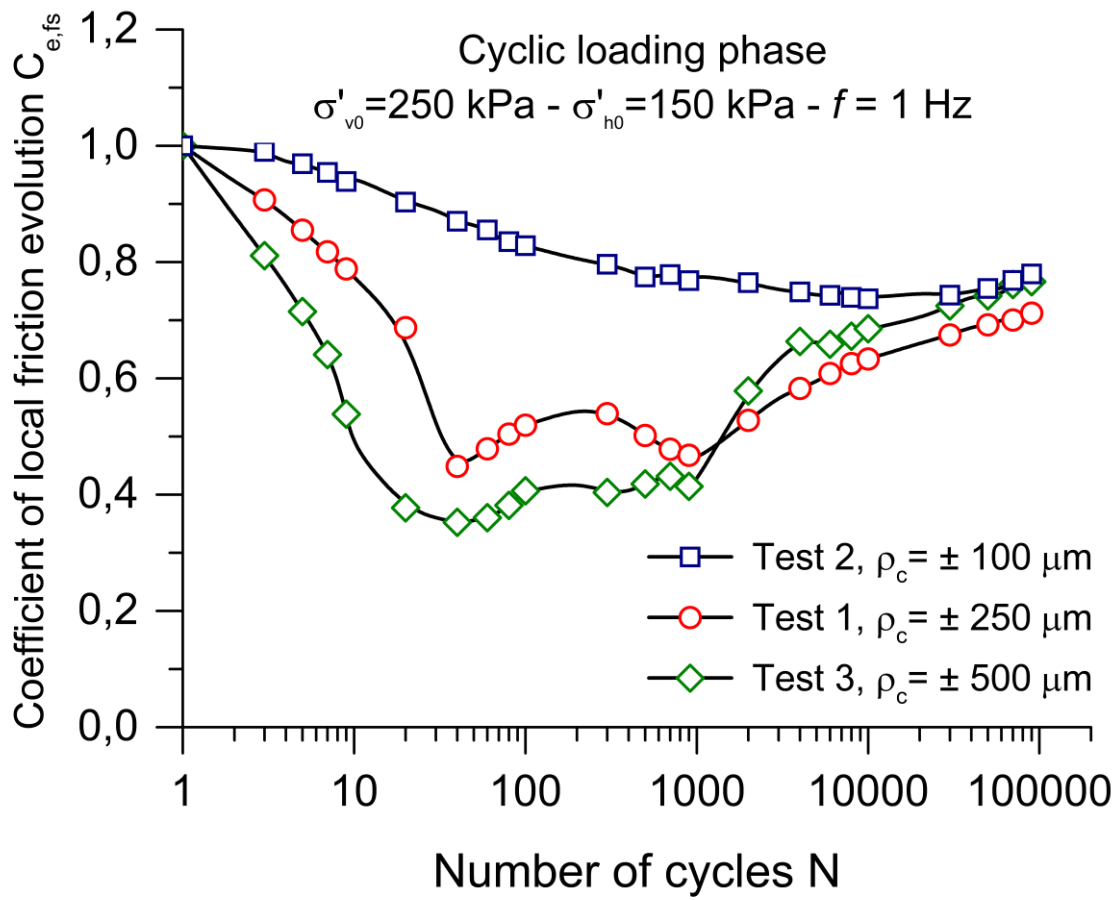


Fig. 11. Influence of the cyclic displacement amplitude on the evolution of local friction upon cyclic loading

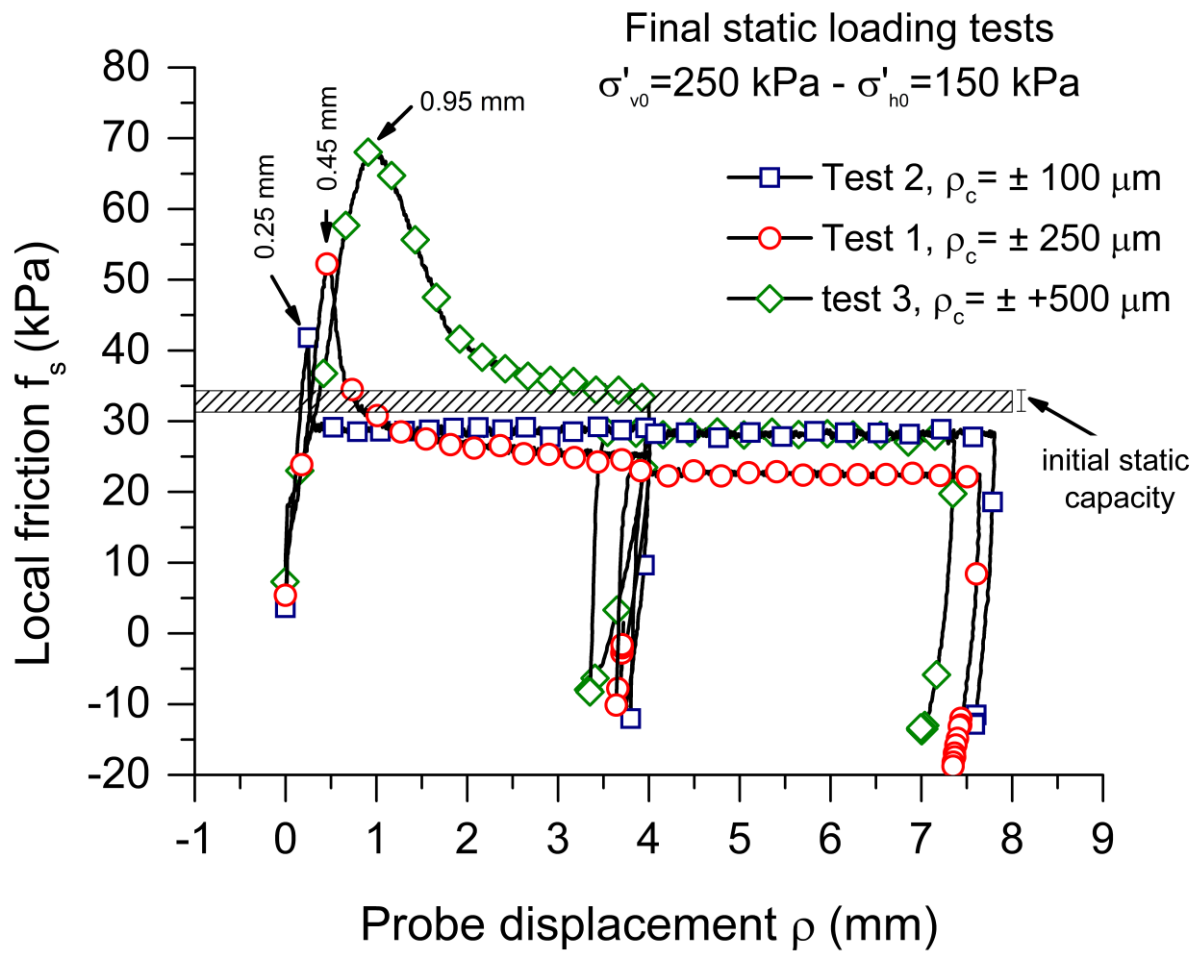


Fig. 12. Influence of cyclic displacement amplitude on the evolution of local friction upon post-cyclic static loadings

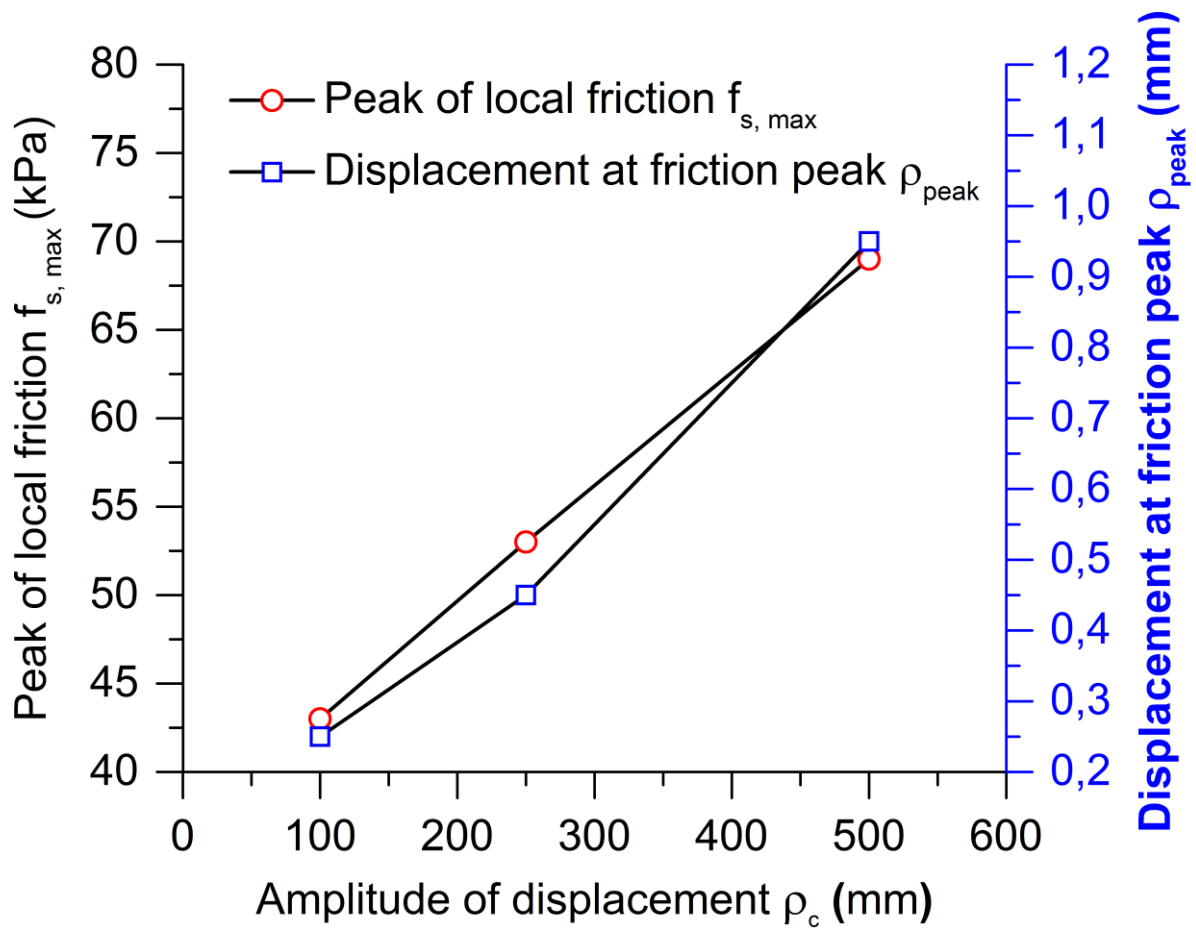


Fig. 13. Influence of cyclic displacement amplitude on the peak of local friction and the necessary displacement to reach the peak upon post-cyclic static loading

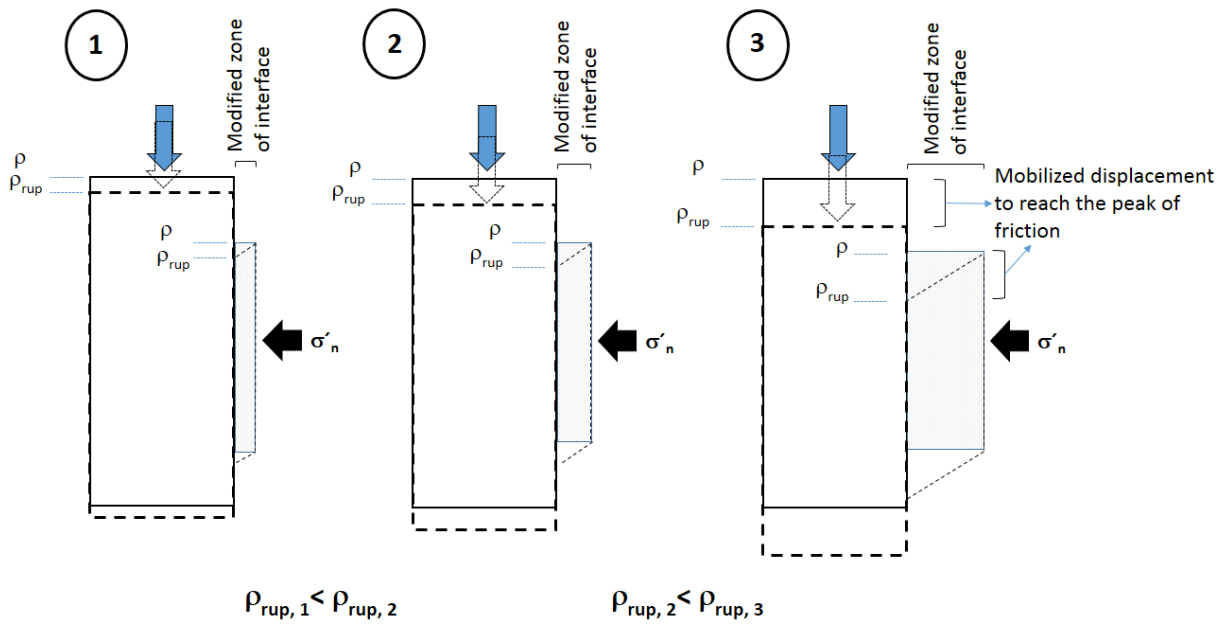


Fig. 14. 2D conceptual scheme of the influence of cyclic displacement amplitude on the modified zone of interface

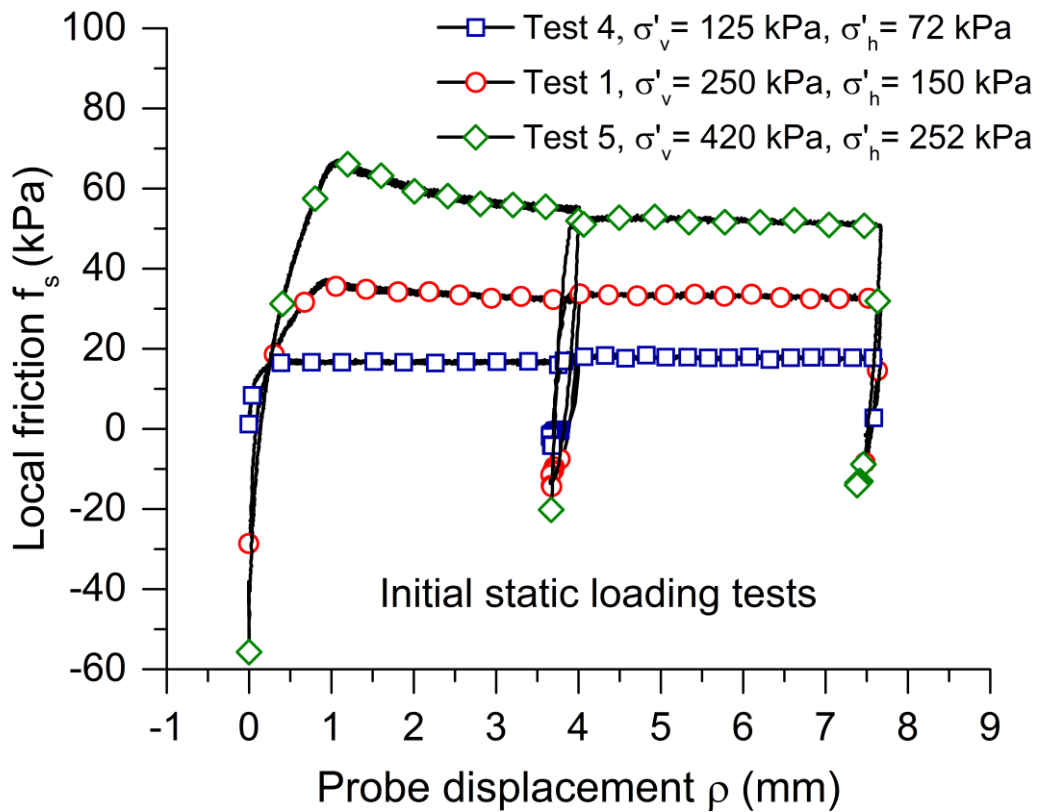
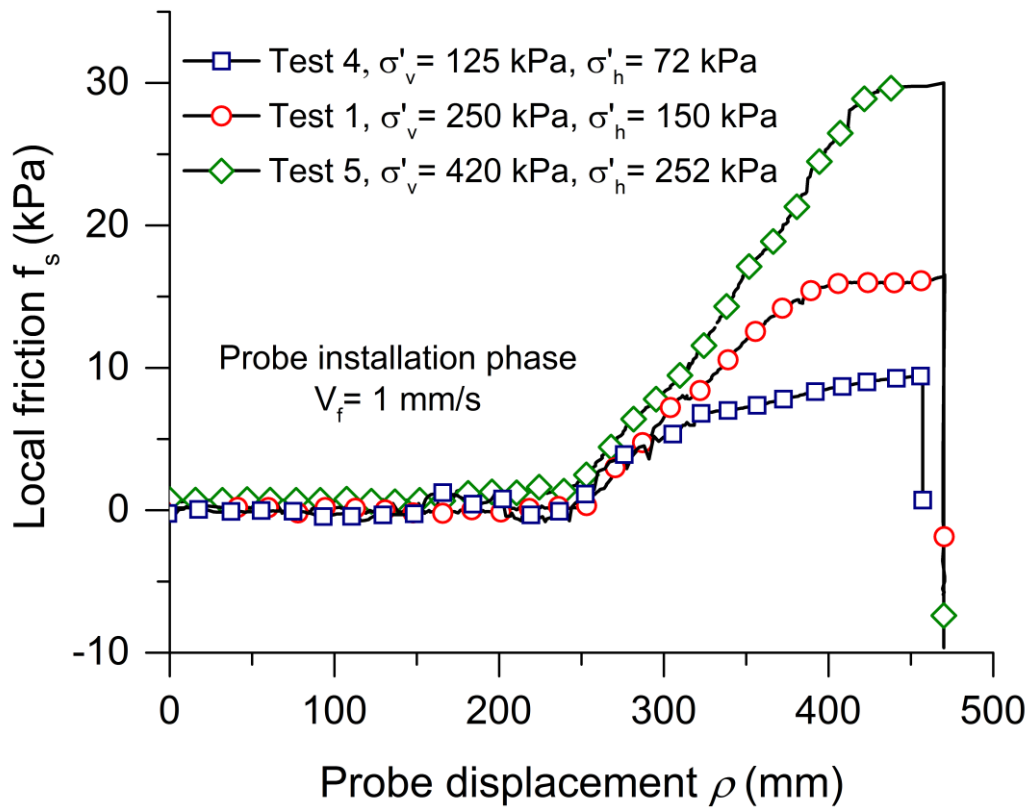


Fig. 15. Influence of initial effective consolidation stress level on the evolution of local friction upon installation and pre-cyclic static loading phases

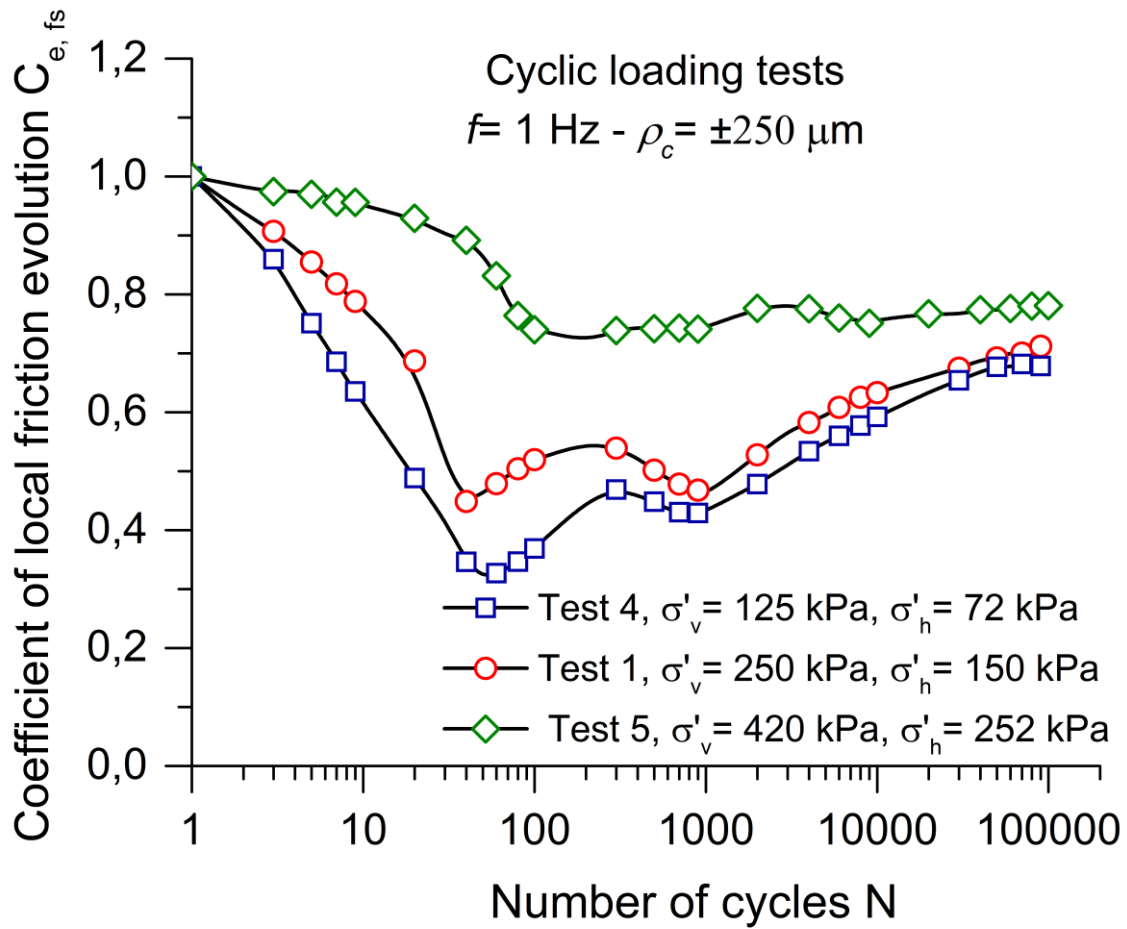


Fig. 16. Influence of initial effective consolidation stress level on the evolution of local friction upon cyclic loading

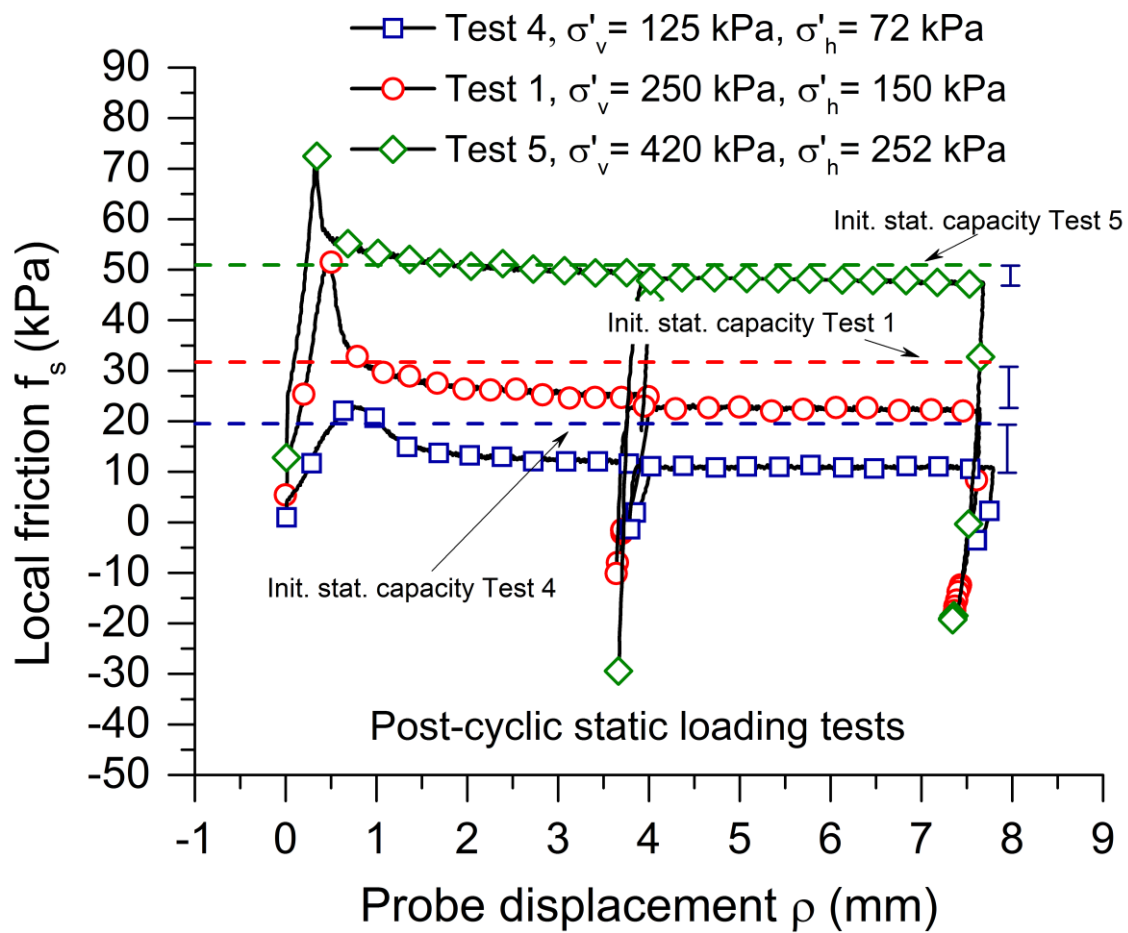


Fig. 17. Influence of initial effective consolidation stress level on the evolution of local friction upon post-cyclic static loading phases

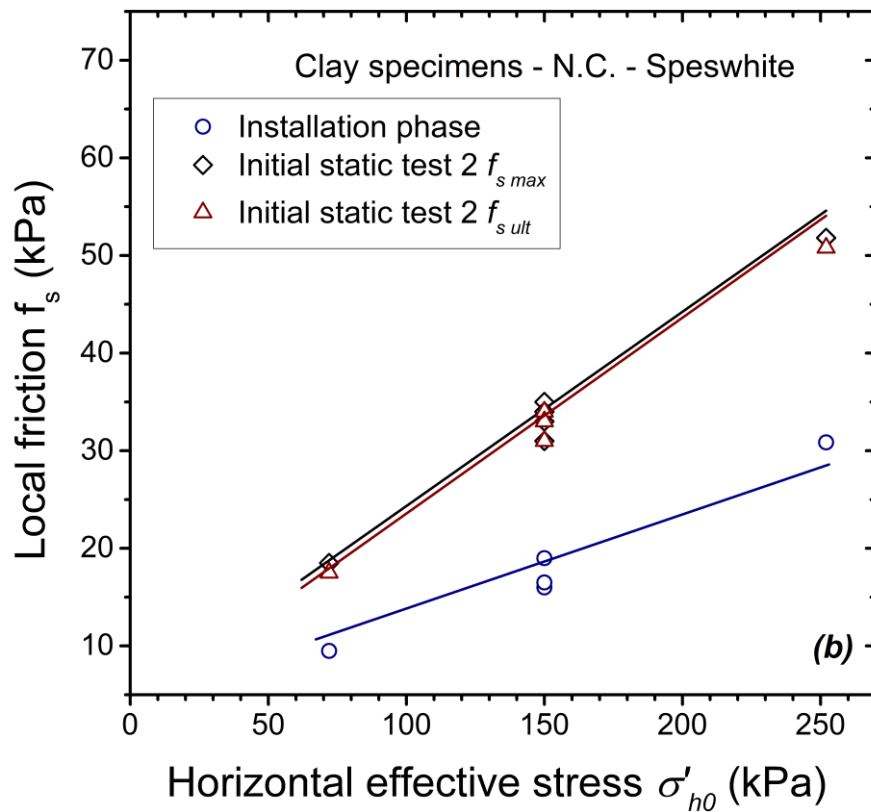
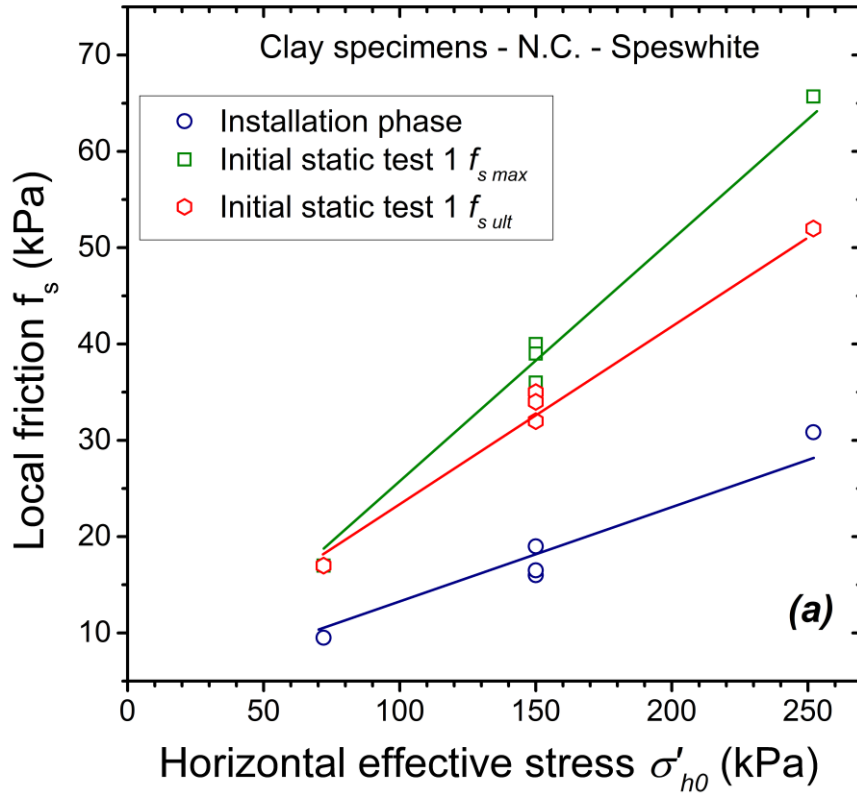


Figure 18. Synthesis of maximum and ultimate values of local friction upon: (a) 1st pre cyclic static tests and (b) 2nd pre cyclic static tests compared to the maximum mobilized friction upon installation phase

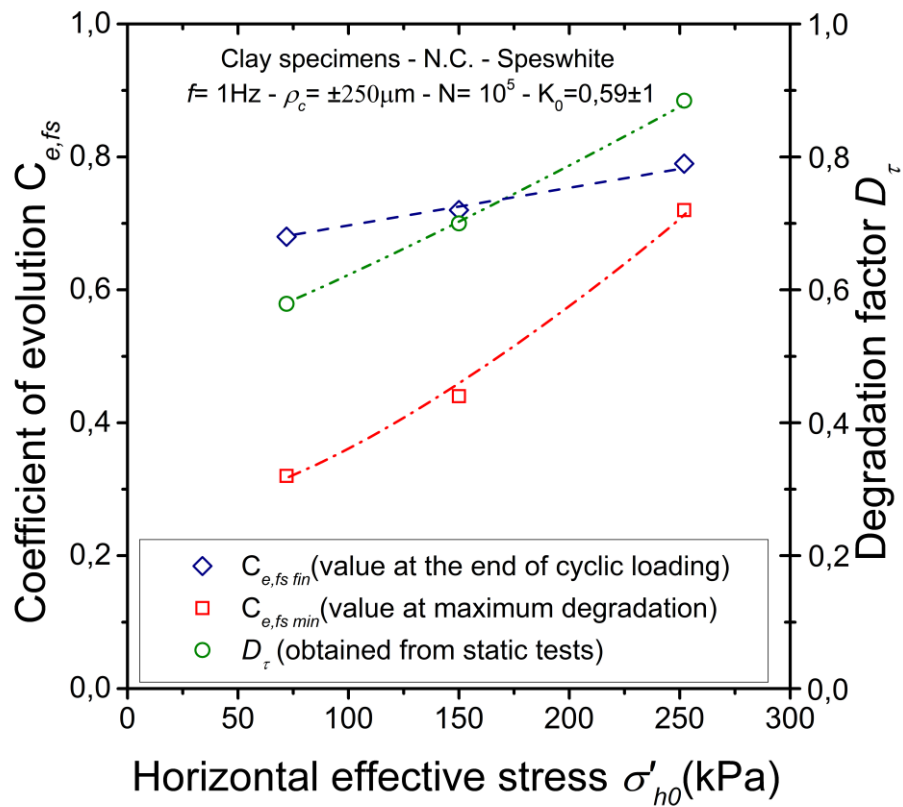
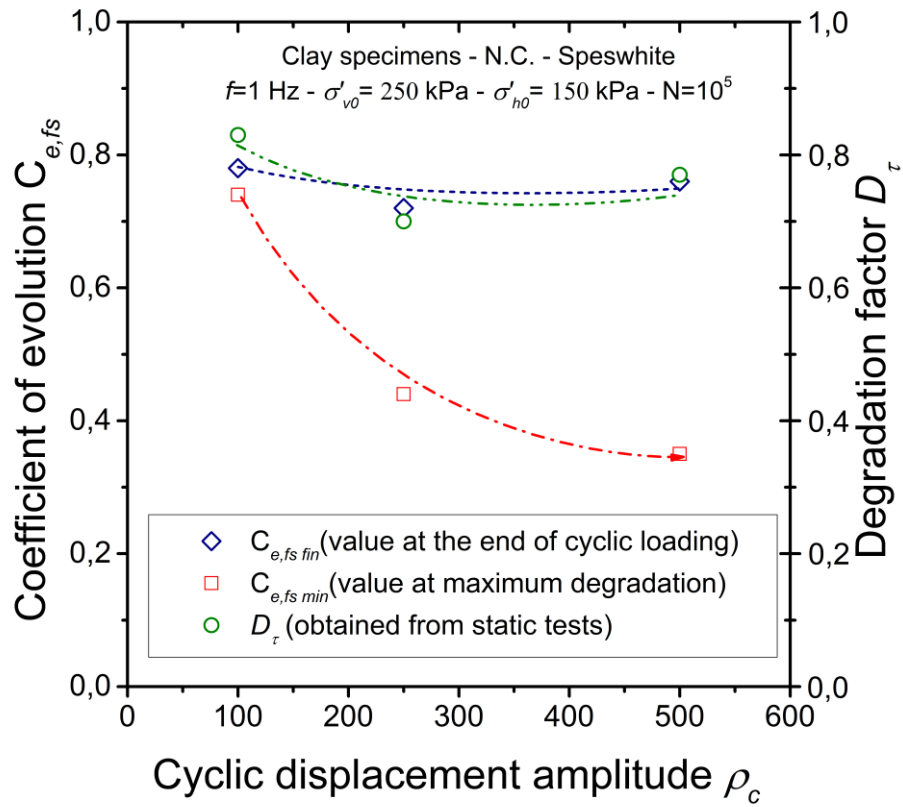


Figure 19. Synthesis of the effect of cyclic displacement amplitude and effective horizontal stress on coefficient of evolution $C_{e,fs}$ and degradation factor D_τ

Evolution of cyclic local friction along clay-pile interface for very large numbers of cycles: parametric study

Tables

Table 1. Physical properties of Speswhite kaolinite

Mineralogy	Liquid limit (%)	Plastic limit (%)	Plasticity index (%)	Specific gravity (g/cm ³)	Percentage finer than 10 μ m (%)
kaolinite	58	28	30	2,64	98

Table 2. Main characteristics of tests performed

Test identification	σ'_{v0} (kpa)	σ'_{h0} (kpa)	Frequency f (Hz)	Cyclic amplitude ρ_c (μ m)	Number of cycles	Observations
Test 1	250	150	1	± 250	100 000	Reference test
Test 2	250	150	1	± 100	100 000	Effect of amplitude
Test 3	250	150	1	± 500	100 000	Effect of amplitude
Test 4	125	72	1	± 250	100 000	Effect of initial state
Test 5	420	252	1	± 250	100 000	Effect of initial state

Table 3. Synthesis of the results in term of coefficient of evolution and the degradation factor

Test identification	σ'_{v0} (kPa)	σ'_{h0} (kPa)	Frequency f (Hz)	Cyclic amplitude ρ_c (μ m)	Number of cycles N	C_{efs}		D_τ
						maximum degradation	at the end of cyclic test	
Test 1	250	150	1	± 250	100 000	0,44	0,72	0,70
Test 2	250	150	1	± 100	100 000	0,74	0,78	0,83
Test 3	250	150	1	± 500	100 000	0,35	0,76	0,77
Test 4	125	72	1	± 250	100000	0,32	0,68	0,58
Test 5	420	252	1	± 250	100000	0,72	0,79	0,88